the general science journal

Evolution From the Complex Plane to the Quaternion Coordinate System to the Trispatial Geometry

André Michaud
Service de Recherche Pédagogique

➔ **Cliquer ici pour version française**
➔ **Haga clic aquí para versión en español**
➔ **Hier anklicken für die Deutsche Fassung**

Abstract: The object of this article is a comparative analysis of the geometric characteristics of the 2D unit vector set of the complex plane as used in Quantum Mechanics and in the treatment of electric LC circuits, of the 3D unit vector set of Hamilton's hypersphere as used in quantum theory and finally of the 3x3D unit vector set of the trispatial geometry as used in electromagnetic mechanics. Analysis of the implications of extending the use of the hypersphere coordinate system to the treatment of LC circuits and to the traditional 3D Cartesian coordinate system, and of the consequences of using a unique property of the vectorial cross product of the quaternion complex unit vectors of reversing the direction of application of the resulting real unit vector in the development of electromagnetic mechanics by means of the trispatial geometry. Then provide a summary of the main fundamental electromagnetic mechanics issues that the use of the quaternion vector cross product in the trispatial geometry allowed resolving, the first of which was the identification of the properties that the fundamental energy must have for it to obey the conditions identified by Louis de Broglie for localized electromagnetic photons to obey Maxwell's equations. And finally, presentation of the main complementary mechanical processes that were developed upon taking into account these properties of the energy substance and this special property of the quaternion vector cross product to explain the cause of electromagnetic frequencies, the relationship between the electron's spin and its magnetic aspect, the decoupling of massless electromagnetic photons into massive electron-positron pairs, the existence of the invariant electric charges for the electron and positron and of the fractional charges of the scatterable internal sub-components of protons and neutrons, the stability of the proton and the instability of the isolated neutron, etc..

Keywords: Complex plane; Quantum Theory; Quaternions; trispatial geometry; electromagnetic mechanics.

This article was published in the IJERD engineering *Journal* in March 2024:

Michaud, A. (2024) *Evolution From the Complex Plane to the Quaternion Coordinate System to the Trispatial Geometry*. International Journal of Engineering Research and Development e-ISSN: 2278-067X, **p**-ISSN: 2278-800X. March 2024. Volume 20, Issue 3. pp. 108-130.

http://www.ijerd.com/paper/vol20-issue3/2003108130.pdf

Equation (26) that did not come out right in the published version is reproduced here for convenience:

$$m_e c^2 \vec{\mathbf{0}} = \left[\frac{\varepsilon_0 \mathbf{E}^2}{2} V\right]_Y \vec{\mathbf{J}}\,\vec{\mathbf{i}} + \left[2\left(\frac{\varepsilon_0 \mathbf{V}^2}{4}\right)_X (\vec{\mathbf{I}}\,\vec{\mathbf{j}}, \vec{\mathbf{I}}\,\vec{\mathbf{j}}) \cos^2(\omega t) + \left(\frac{\mathbf{B}^2}{2\mu_0}\right)_Z \overleftrightarrow{\mathbf{K}} \sin^2(\omega t)\right] V \qquad (26)$$

Other articles in the same project:

INDEX -Electromagnetic mechanics – The 3-Spaces Model

In case the IJERD site is offline, a copy of this paper is available here:

International Journal Of Engineering Research And Development

e- ISSN: 2278-067X, p-ISSN: 2278-800X, www.ijerd.com

Volume 20, Issue 3 (March, 2024), PP. 108-134

Evolution From the Complex Plane to the Quaternion Coordinate System to the Trispatial Geometry

André Michaud

Service de Recherche Pédagogique

Abstract: The object of this article is a comparative analysis of the geometric characteristics of the 2D unit vector set of the complex plane as used in Quantum Mechanics and in the treatment of electric LC circuits, of the 3D unit vector set of Hamilton's hypersphere as used in quantum theory and finally of the 3x3D unit vector set of the trispatial geometry as used in electromagnetic mechanics. Analysis of the implications of extending the use of the hypersphere coordinate system to the treatment of LC circuits and to the traditional 3D Cartesian coordinate system, and of the consequences of using a unique property of the vectorial cross product of the quaternion complex unit vectors of reversing the direction of application of the resulting real unit vector in the development of electromagnetic mechanics by means of the trispatial geometry. Then provide a summary of the main fundamental electromagnetic mechanics issues that the use of the quaternion vector cross product in the trispatial geometry allowed resolving, the first of which was the identification of the properties that the fundamental energy must have for it to obey the conditions identified by Louis de Broglie for localized electromagnetic photons to obey Maxwell's equations. And finally, presentation of the main complementary mechanical processes that were developed upon taking into account these properties of the energy substance and this special property of the quaternion vector cross product to explain the cause of electromagnetic frequencies, the relationship between the electron's spin and its magnetic aspect, the decoupling of massless electromagnetic photons into massive electron-positron pairs, the existence of the invariant electric charges for the electron and positron and of the fractional charges of the scatterable internal sub-components of protons and neutrons, the stability of the proton and the instability of the isolated neutron, etc..

Date of Submission: 10-03-2024 Date of Acceptance: 23-03-2024

I. INTRODUCTION

Recent experiments have clearly demonstrated that the use of *complex numbers* in quantum theory equations is essential to correctly account for the outcome of these experiments and that restricting the calculations to only *real numbers* could not predict as accurately the outcome of these experiments, as reported in a recent *Physics World research update* article [1][2][3].

But given that the set of *real numbers* represented by a is a subset of *complex numbers* $a + \boldsymbol{i}b$ – in which $\boldsymbol{i}=\sqrt{-1}$ and a and b are real numbers – and that the relation between the real part a and the complex part $\boldsymbol{i}b$ is of geometric nature on the *complex plane*, that does not seem to belong to normal space as traditionally mapped over by the 3D (x, y, z) Cartesian coordinate system, but is nevertheless understood as being perpendicular to a *real axis* parallel to the x-axis of the Cartesian coordinate system, a closer look at the geometric aspect of this relationship seems to be in order.

It was Caspar Wessel in 1797 who identified the perpendicular property of the complex plane with respect to the axis of real numbers, as he understood that a directed line segment extending from point zero of the real axis, corresponding to $r=\sqrt{(a^2 + b^2)}$ and set at an angle θ with respect to the real axis, also could be used to represent a *complex number*.

This means that since $r\angle\theta=a + \boldsymbol{i}b$, which implied that when a is set to 0 along the real axis and b is set to 1, then $\boldsymbol{i}=\sqrt{-1}=r\angle 90°=1\angle 90°$ becomes *by structure* a *unit vector* of magnitude 1 rotated by 90° from the real axis along an *imaginary axis* exactly perpendicular to the real axis, the latter being seen as parallel to the x-axis of the Cartesian coordinate system, but which is neither the y-axis nor the z-axis of this coordinate system, even if this imaginary axis is often represented as coinciding with the Cartesian y-axis for convenience of graphic representation. See further on **Figures 1** and **2** and for more further on Wessel's reasoning in defining this geometric orientation of $\boldsymbol{i}$ with respect to the real axis, as put in perspective in Reference [4].

It's also worth noting that the *hypercomplex numbers* $a + \boldsymbol{i}b + \boldsymbol{j}c + \boldsymbol{k}d$ defined by Hamilton, in which $\boldsymbol{j}$ and $\boldsymbol{k}$ are also equal to $\sqrt{-1}$ – and can likewise be defined as unit vectors *by structure*, just like $\boldsymbol{i}$ – have been extensively associated with quantum theory from the *algebraic* perspective by many researchers, for example [5][6], and also to electromagnetic theory [7][8], but not from the *geometric* perspective that will be addressed

here.

Another domain that also makes use of complex numbers is the analysis of sinusoidally driven electronic circuitry, typically involving RLC or LC systems made of wire coils and capacitors – R standing for *resistance*, L standing for *magnetic inductance* and C standing for *electric capacitance* – whose characteristics establish the signal frequencies required in these circuits [9].

A note of interest at this point regarding LC systems, is that such an electromagnetic relation can also be related to the de Broglie double-particle electromagnetic photon when Maxwell's *displacement current* is applied in the establishment of their inner electromagnetic structure as they propagate in vacuum at the subatomic level of magnitude [10][11], in which the permittivity constant of vacuum ε_0 is in reality a measure of *transverse electric capacitance per meter* – also symbolized by C in electromagnetic theory. On its part, the permeability constant of vacuum μ_0 is measure of *transverse magnetic inductance per meter* – also symbolized by L in electromagnetic theory [12].

It is to be noted here also that hypercomplex numbers apparently never were related to LRC or LC systems from the geometric perspective either, despite the clear involvement of complex numbers in their equations. We will see further on that hypercomplex numbers can be geometrically involved in LRC and LC systems, although in a potentially unexpected manner.

In summary, in light of the results of experiments [1] and [2], it can be said that *something* in the equations of Quantum Mechanics and of RLC and LC systems is *perpendicular by structure* to *something else*, in a manner that cannot be discounted without losing precision in the experiments, that confirm the requirement for use of complex numbers in these equations. We will explore in this article what these "somethings" may turn out to be.

Finally, we will examine the relation between the trispatial geometry that underlies the electromagnetic mechanics of elementary particles [13][14] and these complex geometric relations when the standard set of $\boldsymbol{i}=\boldsymbol{j}=\boldsymbol{k}=1$ unit vectors *by definition* is replaced by the set of complex unit vectors *by structure* $\boldsymbol{i}=\boldsymbol{j}=\boldsymbol{k}=\sqrt{-1}=1\angle 90°$ in the 3D Cartesian coordinate system and in the coordinate system of the trispatial geometry.

II. HISTORICAL PERSPECTIVE

Let us first examine how de Broglie's *pilot wave* concept – that he initially named *phase wave* in his 1924 thesis [15][16] – and the introduction of complex numbers by Schrödinger in his wave equation [17], modified the early 20th century traditional classical mechanics perception of the electron as possibly being a very small localized rigid body with a fixed rest mass moving on a precise closed trajectory in the hydrogen atom, towards a much less clearly defined state of localization and motion.

Here is the quote of the metaphorical comparison that he proposed in his 1924 thesis to illustrate this motion of the electron as he visualized it in the idealized Bohr model of the hydrogen atom:

> *"The notion of phase wave will allow us to provide an explanation of Einstein's condition. It results from the considerations of Chapter II that the trajectory of the mobile is one of the rays of its phase wave, the latter must run along the trajectory with a constant frequency (since the total energy is constant) and a variable velocity whose value we have learned to calculate. Propagation is therefore analogous to that of a liquid wave in a channel closed on itself and of variable depth. It is physically evident that to have a stable regime, the length of the channel must be in resonance with the wave. In other words, the wave portions that follow each other at a distance equal to an integer multiple of the length l of the channel and that are therefore at the same point in the channel, must be in phase. The resonance condition is $l = n\lambda$ if the wavelength is constant and $\oint (v/V)\, dl = n$ (integer) in the general case."*
>
> Louis de Broglie (1924) ([16], p. 51)

He then proposed the following kinematic mechanics equation that triggered the development of Wave Mechanics soon followed by Quantum Mechanics ([16], p. 52):

$$m_0 \oint v \cdot dl = 2\pi R\, m_0 v = n\, h \tag{1}$$

See **Section 6** of References [13][14] for complete analysis of this seemingly unremarkable equation that so revolutionized fundamental physics when Erwin Schrödinger converted it into a vectorial wave mechanics equation:

$$i\hbar \frac{\partial}{\partial t} \Psi(\vec{r},t) = \left[-\frac{\hbar^2}{2m} \frac{\partial^2}{\partial x^2} + V(\vec{r},t) \right] \Psi(\vec{r},t) \tag{2}$$

Schrödinger's Equation (2) generates the exact same sequence of integer related quantized momentum

energy levels as de Broglie's Equation (1), but now calculated from a wave oscillation perspective rather than from the classical mechanics kinematic perspective used by de Broglie of a localized electron mass radially oscillating about the idealized circular trajectory of the ground state of the Bohr model of the hydrogen atom.

The Bohr atom ground state circular trajectory is termed *idealized* because its theoretical establishment about the central proton was initially assumed to be run by a localized electron seen as massive in the traditional classical mechanics sense, but that de Broglie had recently understood as having to be captive in an oscillating radial resonance state about this circular orbit for the integer related sequence of frequencies observed in the hydrogen atom spectrum to be explainable.

The further away metastable *orbits* of the Bohr atom that the electron was assumed to jump to when energized away from the ground state *orbit* could then be explained as being resonance multiples of the length of the ground *orbit*, directly explaining the whole spectrum of energy frequencies emitted by the hydrogen atom as the electron returns to the ground state from this series of metastable distances, corresponding to the Lyman series.

The major difference between Equation (1) and Equation (2) was the introduction by Schrödinger of complex numbers in Equation (2), that involves a structural perpendicular relation between some elements of wave mechanics Equation (2), that are absent from de Broglie's classical mechanics Equation (1).

Let us now consider what elements of de Broglie's conclusion about the radial oscillation of the electron about the idealized ground state circular orbit of the Bohr model that Schrödinger must have perceived as being perpendicular to each other, to the extent of being representable by complex numbers.

From his own stated conclusion, de Broglie obviously perceived the oscillation of the electron along its trajectory as involving a longitudinal momentum pulse – his phase wave as quoted above that he eventually also referred to as a pilot wave – that would propel the electron, which would result in a stable standing transverse oscillation of the electron similar to the classical mechanics lineic mass of an elastic cord being swung up and down transversely as the initial pulse progresses longitudinally along the cord [12].

This observation alone totally justified the introduction by Schrödinger of the complex condition $z=\cos\theta + \boldsymbol{i} \sin\theta$, in his Equation (2) representing the electron *rest mass* as a weakly localizable *diffuse representation of presence probability* [See Equation (4)] involved in a dynamic transverse motion by adapting the free particle wave function Equation (3), in which $\boldsymbol{i}$ establishes that this motion of the electron, whose *center-of-presence* is represented by point P in **Figure 1** now has to oscillate *by structure* perpendicularly to the Bohr trajectory in de Broglie's Equation (1), with the Bohr idealized ground state orbit now conceptually becoming a circular close circuit *x-axis* of the complex plane, on which plane the electron would cyclically oscillate from outside to inside the Bohr orbit in standing mode.

$$\Psi(\vec{r},t) = \cos(k\vec{r} - \omega t) + i\sin(k\vec{r} - \omega t) \tag{3}$$

But since the complex plane is not conceptually restricted to be established strictly on the same plane as the circular ground state trajectory, but can have any transverse angular orientation about this trajectory, Equation (2) also defines a cylindrical volume about the ground state trajectory related to the $\boldsymbol{i} \sin(kx - \omega t)$ amplitude of the phase wave, a volume within which the electron is likely to be located at any point in space at any given moment within this volume, as put in perspective in References [18][19], and inside which Heisenberg's statistical method could be directly mapped. The resulting uncertainty of the instantaneous position of the electron within this volume at any given moment can possibly be what caused Heisenberg to come up with his *Uncertainty principle*.

This is why it was suggested in 2013 in Reference [20] to restrict the probabilistic spread of the possible locations of the electron in motion in the ground state of the isolated hydrogen atom to the limits of this cylindrical volume instead of extending it to + and - ∞, to account for the limits imposed by the inertia of the electron during its transverse acceleration and deceleration sequences as it oscillates about the mean Bohr radius, with the set of most probable locations averaging out at the Bohr radius :

$$\int_{r}^{R} \left|\Psi_{(x,t)}\right|^2 dVdt = 1 \tag{4}$$

Of course, due to interactions with surrounding matter, this cylindrical volume is likely in reality to spread at the limit to a 3D volume circumscribed by the surfaces of two concentric spheres whose inner and outer radii will respectively be r and R on either side of the Bohr radius. Consequently, it is to this volume exclusively, accounted for by the product of its complex function with its conjugate $\Psi^*\Psi$ in Equation (4), that the normalization condition should apply, any other localization in space becoming physically impossible for the electron in the ground state of the hydrogen atom due to its inertia.

As previously mentioned, Schrödinger thus introduced with his equation a characteristic that never was related before to the motion of massive bodies, that is, a perpendicular relation between the local transverse

motion of the electron mass about its assumed trajectory in the Bohr atom and the direction of motion of the phase wave energy that carries it. This perpendicular relation is introduced by symbol ***i***, named the *imaginary unit*, equal to $\sqrt{-1}$ – actually a unit vector defined as $1\angle 90°$ with respect to the real axis of the complex plane, as defined by Vessel, as explained further on – which, when squared ($\boldsymbol{i}^{\,2}$) resolves to -1, which reverses the direction of application of the related vector, which is the added benefit of using ***i*** in vectorial equations.

As previously mentioned, complex numbers can always written under the form:

$$z = a + bi \tag{5}$$

This means that to locate a point **P** in the 2D coordinate system of the complex plane, a first displacement is required to the right by a distance *a*, measured in real numbers, from the origin of a horizontal axis (**Figure 1a**), and that ***i*** reveals that a second displacement by a distance *b*, also measured in real numbers, must be made *at right angle* from the rightmost end of line segment *a*, which will lead to a location outside the volume of normal space mapped over by the Cartesian 3D coordinate system, where point **P** will be located.

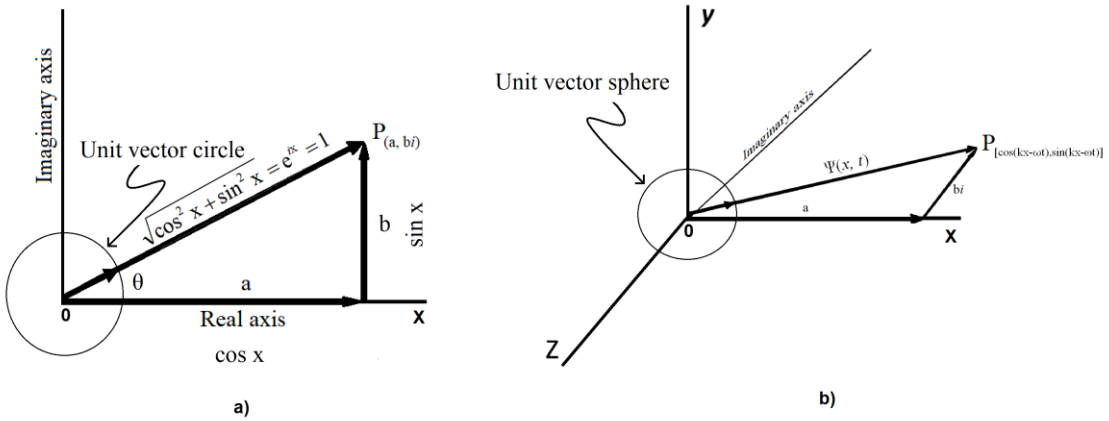

Figure 1: *Real* and *imaginary* axes of the complex plane.

Our purpose here however is not to analyze in any more depth the Schrödinger equation, which is explained in detail in numerous textbooks, such as the outstandingly well made Reference [21], but to explore further the very special property of $\boldsymbol{i}=\sqrt{-1}$ acting as a *static geometric rotation operator* of any vector representation of whatever quantity has a magnitude and a direction of application with respect to the origin *O* of the 2D complex plane, such as force, pressure, velocity, etc., as put in perspective in Reference [4].

The consequence of this new wave representation of the electron introduced by Schrödinger was that its presence in the hydrogen atom began to be seen as involving spread out *orbitals*, of which the idealized circular orbits of the Bohr model end up representing the set of mean distances from the proton at which each resonance volume is established with Equation (2).

It now turns out that de Broglie was right in hypothesizing that some sort of *carrying energy wave*, that he first named a phase wave, and then a pilot wave, was propelling and guiding the rest mass of the electron, and that Schrödinger was right in concluding that the *momentum energy* that he related to this pilot wave was acting perpendicularly to the energy of which the rest mass of the electron was made, but in a manner that became clear only much later as we will see further on, according to conditions that de Broglie identified himself in 1937 [22] for this carrying energy to obey Maxwell's equations, according to a space geometry that needed to extend beyond the frame of continuous 4D space-time:

> *"... la non-individualité des particules, le principe d'exclusion et l'énergie d'échange sont trois mystères intimement reliés : ils se rattachent tous trois à l'impossibilité de représenter exactement les entités physiques élémentaires dans le cadre de l'espace continu à trois dimensions (ou plus généralement de l'espace-temps continu à quatre dimensions). Peut-être un jour, en nous évadant hors de ce cadre, parviendrons-nous à mieux pénétrer le sens, encore bien obscur aujourd'hui, de ces grands principes directeurs de la nouvelle physique."*
>
> Louis de Broglie 1937 ([22], p. 273)

> *"... the non-individuality of particles, the exclusion principle and exchange energy are three intimately related enigmas; all three are tied to the impossibility of exactly representing elementary physical entities within the frame of continuous three dimensional space (or more generally of continuous four dimensional space-time). Some day maybe, by escaping from this frame, will we better grasp the meaning, still quite cryptic today, of these major guiding principles of the new physics."*

This expanded space geometry envisioned by de Broglie was presented at Congress-2000 in July of year 2000 [23], and a discovery made by Paul Marmet in 2003 [24][25] about the magnetic field of the accelerating electron allowed understanding that de Broglie's pilot wave had the exact same internal electromagnetic structure as the double-particle photon whose conditions of establishment that he identified in 1937, which equation was formally published in 2016 [10][11] explaining the relation between the electron carrier-photon and the free moving double-particle electromagnetic photon that de Broglie had hypothesized in 1937, after having been established as the electron carrier-photon in 2013 [26].

Going even further that the already daring curving to a closed circle the traditionally perceived as rectilinear complex plane real axis illustrated with **Figure 1**, as introduced by Schrödinger, we will see further on how the trispatial geometry allows locating this axis at the center-of-presence of the electron *rest mass energy*, which allowed rotating the direction of application of its momentum energy directly towards the proton, instead of being oriented along the idealized Bohr ground state circular trajectory as understood at the beginning of the 20th century, as accounted for by the Coulomb restoring force in attractive action between the negatively charged electron and the positively charged proton, to act in counter-pressure against the permanent mutual magnetic repulsion between the electron and the proton due to their default parallel magnetic spin alignment [18][19] as confirmed by the foundational experiment that underlies the development of the trispatial geometry [20] and that explains the stability of the hydrogen atom, to mechanically explain why the electron does not even need to be in orbit about the proton to stabilize at the known Bohr radius mean distance from the proton, as analyzed in References [18][19].

We will examine this expanded space geometry further on, but let us first completely put in perspective what has been established with regard to complex numbers, the complex plane, hypercomplex numbers and the *quaternion structure*, before examining the second domain in which complex numbers and the complex plane found a practical application, that of RLC and LC systems and see if they account as completely as expected for these well known electromagnetic processes as they do for the Schrödinger equation.

III. THE COMPLEX PLANE

In the standard classical mechanics 3D Cartesian coordinate system, the notation symbols ***i***, ***j*** and ***k*** are used to designate the triply orthogonal unit vector set with values ***i=j=k***=1, related to the x-, y- and z-axes of the standard 3D coordinate system illustrated with **Figure 2**, which can lead to some confusion with their use also representing other quantities in different mathematical contexts, which contexts are typically sufficient to establish their local meaning; particularly in the cases of the ***i*** and ***j*** symbols, that in different contexts are both defined with value ***i=j***=√-1, with ***i*** and ***j*** not even coinciding with the geometric x-axis of **Figure 2**.

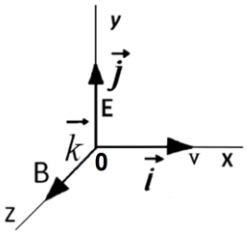

Figure 2: The three perpendicular axes of the Cartesian coordinate system that allow the localization of any (x, y, z) point in space with respect to location **0** set at the center-of-presence of any body or particle in normal space.

The set of symbols ***i=j=k***=1 is traditionally used to identify the unit vector set related to the Cartesian coordinate system. However, they are also used with a different definition as *complex* unit vectors ***i=j=k***=√-1 in relation with *complex* and hypercomplex numbers.

Complex numbers are used in Quantum Mechanics as we have just seen and are also extensively used in the electrical domain, in particular in the set of equations related to *inductance* L and *capacitance* C that we will study here, in which ***j***=√-1 is substituted to ***i***=√-1 to avoid confusion with the symbol for current, which is also symbolized with ***i***. We will see further on how the quaternion ***i=j=k***=√-1 unit vector *set* can also be related to *inductance* and *capacitance*, which is an exercise that seems not to have been attempted before, despite the potential benefits of correctly relating the energy involved in LC oscillation to the well known perpendicular electromagnetic relation between the ***E***-field related to the C-phase and the ***B***-field related to the L-phase of LC oscillation, instead of the only relation at 180° allowed between them in the complex plane as illustrated with **Figure 3**, even if they both are representable as 90° correctly offset with respect to the real axis.

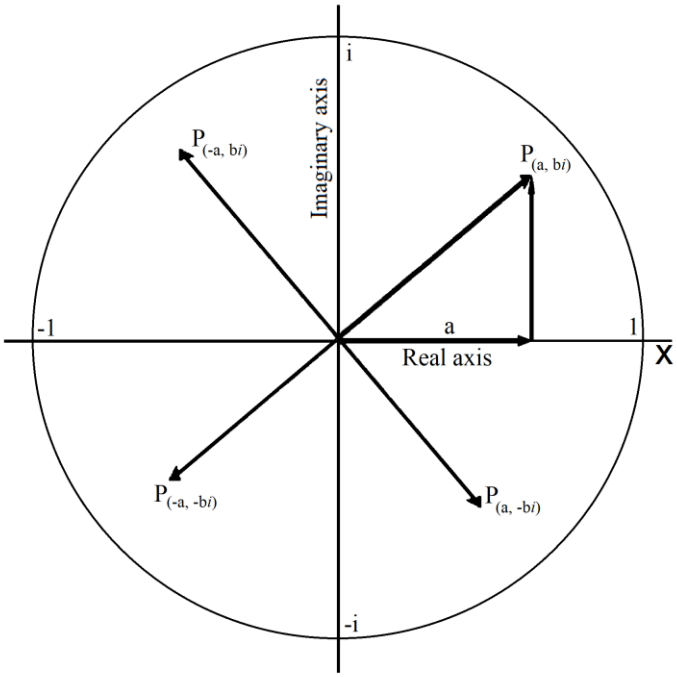

Figure 3: The unit vector circle of the complex plane.

As also illustrated in **Figure 2**, the triply perpendicular electromagnetic relations ***E/B*=c** and ***E/B=v*** are also mapped into the same 3D Cartesian coordinate system to illustrate the fact that the vector cross product of mutually perpendicular ***E***-field and ***B***-field generates a velocity vector perpendicular to both the ***E***-field and the ***B***-field, with the x-axis taken as the axis along which the motion of the corresponding electromagnetic energy will occur.

The center of the coordinate system – location **0** of all three axes – can be located at the center-of-presence of any given object, towards which or away from which vectors could be pointing.

What is particularly intriguing about the ***i***=√*-1* unit vector used on the complex plane is that although its origin coincides with the center of the 3D Cartesian coordinate system, the vector itself does not point to any (x, y, z) location within our familiar 3D-space, but rather points to a location on a 2D (x, ***i***) plane which is perpendicular to this coordinate system along a so-called imaginary axis, a plane that was named the complex plane for this reason, which is typically represented with **Figure 1a**.

To illustrate more visually how this complex plane and its imaginary axis are oriented with respect to the x-axis of the standard coordinate system, and by the same token also with respect to the other two axes, **Figure 1b** visually rotates the **Figure 1a** representation sidewise by 90° about the x-axis to illustrate that it is oriented in a fourth direction perpendicular to the other 3 axes, which is very difficult to mentally come to terms with, given that dealing with more than 3 perpendicular spatial axes doesn't seem to make any logical geometric sense, because as illustrated with **Figure 3**, after having rotated 3 times by 90° starting from a given angle set as a 0° angular location on a given plane, rotating a fourth time by 90 ° can only bring us back to our starting location of this plane, unless this rotation becomes oriented perpendicularly to this plane.

And when 3 planes are themselves perpendicular to each other as in the Cartesian coordinate system shown in **Figure 2**, a 4 fourth rotation such as exemplified with **Figure 1b**, can only lead *out of normal space*. We will address this issue in a logical way further on. Let's now refresh on a few basic rules that govern the complex plane before proceeding further.

Figure 3 represents the unit vector circle of the complex plane as being rotated 90° about the x-axis, so the plane faces the reader. On this plane, a vector quantity is resolved into two components at right angle to each other, one component *a*, whose direction is along the horizontal x-axis, referred to as the axis of reals, and the other component *b*, extending at right angle with respect to the axis of reals in a direction parallel to the *axis of imaginaries*.

A positive vector having its direction along the x-axis becomes negative if multiplied by -1, i.e. (1·-1=-1), meaning that it will be pointing to the left in **Figure 3**. A positive vector having its direction upwards along the imaginary axis becomes negative if multiplied by -1, i.e. (***i***·-1=√-1·-1=-***i***) and will point downwards along the imaginary axis.

Increasing powers of ***i*** amounts to rotating the related vector counter clockwise on the complex plane

by as many 90° angles ($\boldsymbol{i}^0=1$, $\boldsymbol{i}^1=\boldsymbol{i}$, $\boldsymbol{i}^2=-1$, $\boldsymbol{i}^3=-\boldsymbol{i}$). Further increasing or decreasing powers of ***i*** simply repeat the same 1, ***i***, -1, -***i***. cycle about the origin of the unit vector circle on the complex plane. For this reason, (***i***=√-1) is often named the *rotation operator* [4].

What is very special about this *rotation operator* is that, for example, when a *complex number* such as Equation (5), resolved as **P** in **Figure 1a**, is multiplied by ***i***, both segments *a* and *b* are rotated 90° counter clockwise, locating point **P** in the second quadrant:

$$P = \boldsymbol{i} \cdot z = \boldsymbol{i} \cdot (a + \boldsymbol{i}b) = \boldsymbol{i}a - b \tag{6}$$

Repeated multiplication of the result of the rotation shown in Equation (6) will result in the eventual completion of the full circle about the origin of the complex plane, that is, (*-a* - ***ib***), locating point **P** in the third quadrant, then (*a* - ***ib***) locating it in the fourth quadrant, and finally (*a* + ***ib***), locating it back in the first quadrant.

As mentioned in Introduction, in 1797, Caspar Wessel published a memoir in which he introduced the polar form of complex numbers, from which he succeeded in mathematically explaining why a unit vector with value √-1 geometrically represents a vector segment of length 1 pointing straight up along the imaginary axis of the complex plane.

Given two line segments extending from origin **0** on the complex plane at different angles with respect to the real axis, Wessel established that multiplying the lengths of the two line segments and adding the two angles, with the lengths always taken as positive values, then these two operations determine the length of the resulting line segment and its direction angle with respect to the real axis, and that it is this definition of a product that gives us the explanation of what √-1 means geometrically.

His reasoning was as follows, quoted from Reference ([4], p.53):

> *"Suppose that there is a directed line segment that represents √-1, and that its length is l and its direction angle θ. Mathematically then, we have √-1=l∠θ. Multiplying this statement by itself, i.e., squaring both sides, we have -1=l²∠2θ or, as -1=1∠180°, then l²∠2θ=1∠180°. Thus, l² =1 and 2θ=180°, and so, l=1and θ=90°. This says that √-1 is the directed segment of length one pointing straight up along the vertical axis:"*

$$\boldsymbol{i} = \sqrt{-1} = 1\angle 90^\circ \tag{7}$$

From the geometric perspective, the symbol ∠ simply means "*at rotated angle*".

His grounding hypothesis was established in reference to **Figure 1a**, as explained by Nahin in Reference [4]. So, if $\theta = \tan^{-1}(b/a)$, then:

$$a + \boldsymbol{i}b = \sqrt{a^2 + b^2}\{\cos(\theta) + \boldsymbol{i}\sin(\theta)\} \tag{8}$$

The value of $\sqrt{(a^2+b^2)}$, which is the length of the *radius vector*, is named the *modulus* of *complex number* $a+\boldsymbol{i}b$, and the value of the polar angle $\tan^{-1}(b/a)$ is named the *argument* of $a+\boldsymbol{i}b$. So, in terms of the length of the *radius vector* from the origin to point $a+\boldsymbol{i}b$, multiplying two different directed line segments lead to:

$$a + \boldsymbol{i}b = \sqrt{a^2 + b^2}\angle \tan^{-1}\left(\frac{b}{a}\right) \tag{9}$$

So we now have a perfectly logical explanation of why ***i***=√-1 is a unit vector rotated 90° from the real axis in **Figure 1a**. But when matching the real axis with the x-axis of the 3D Cartesian coordinate system as in **Figure 1b**, we also observe that the imaginary axis along which unit vector ***i*** is oriented, is not the y-axis of the Cartesian coordinate system, and is rather also perpendicular to it.

In summary, there are at least 4 ways to express a *complex number*:

$$z = a + \boldsymbol{i}b,\ z = \mathrm{r}\cos(\theta) + \boldsymbol{i}\mathrm{r}\sin(\theta),\ \mathrm{z} = \mathrm{re}^{\boldsymbol{i}\theta},\ \mathrm{z} = \mathbf{r}\angle\theta \tag{10}$$

The exponential function e^z is related to complex numbers via Euler's formula:

$$e^{\boldsymbol{i}y} = \cos y + \boldsymbol{i}\sin y \tag{11}$$

Well explained in introductory textbooks on complex analysis [27].

IV. THE 3 PERPENDICULAR COMPLEX PLANES OF THE HAMILTON HYPERSPHERE

As noted by Nahin in Reference [4], this is what brought Hamilton to wonder what would emerge from introducing such *rotated* unit vectors within 3D-space as mapped over by the Cartesian coordinate system. This

is what led him to his discovery of quaternions in 1843, which are, hypercomplex numbers, that have the form:

$$H = a \cdot 1 + b \cdot \boldsymbol{i} + c \cdot \boldsymbol{j} + d \cdot \boldsymbol{k} \tag{12}$$

In which a extends on the real axis as in complex plane equation z = a + **i**b and in which [b**i** + c**j** + d**k**] are the three rotated unit vectors of the quaternion coordinate system.

We are entering here the domain of hypercomplex geometry, that involves a coordinate system involving three unit vectors similar to those of the traditional 3D Cartesian coordinate system of **Figure 2**, but that involves the set **i=j=k**=1∠90°, each unit vector **i**, **j** and **k** being perpendicular by structure to the other two, instead of the set **i=j=k**=1 that are mutually perpendicular only by definition, and that now define 3 mutually perpendicular complex planes, the xy-plane, the yz-plane and the xz-plane within the hypersphere thus defined (**Figure 4**).

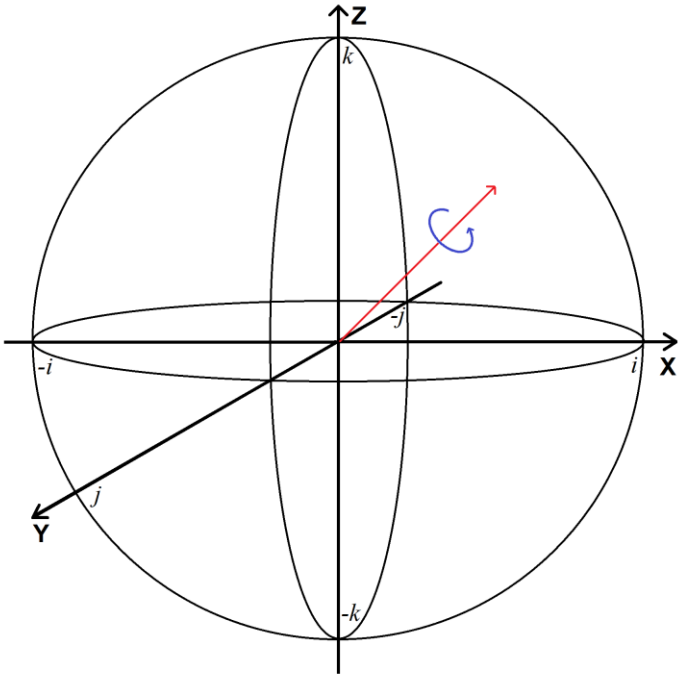

Figure 4: The quaternion coordinate system.

In so doing, Hamilton made a huge step by growing the complex mathematical domain from *one 2D* complex plane on which a vector of any length anchored to the origin **0** of the related 2D coordinate system could be rotated at any possible angle as illustrated in **Figure 3**, to a *three mutually perpendicular* complex planes configuration that now allow rotating the real axis itself at any omnidirectional angle within the hypersphere as illustrated in **Figure 4**.

Whereas the complex plane (**Figure 3**) is divided into 4 quarter circles, the hypersphere (**Figure 4**) is divided into 8 quarters of half-spheres. Four making up the upper half-sphere and four making up the lower half-sphere, with the *xy-plane* having been taken by convention as the default separator between the two half-spheres, and within which hypercomplex numbers such as Equation (12) can orient and rotate a point of the real axis in all directions within the hypersphere, which is a feature extensively used in computer graphics programming, for example.

V. THE QUATERNION 3D COORDINATE SYSTEM

We will not be discussing here this well known ability of quaternions to rotate vectors in a quite useful manner, but will rather analyze an aspect of the ***i***=***j***=***k***=√-1=1∠90° quaternion coordinate system that seems not to have drawn much attention in the mathematical community, nor in the physics community for that matter, despite the known usefulness of the imaginary unit ***i***=√-1 and of the complex plane in resolving capacitance and induction RLC equations in electronic circuits design [28].

To begin addressing this issue, we need to first isolate the quaternion coordinate system from the real axis. This can be done by setting *a* to zero in Equation (12). The triply perpendicular ***ijk*** 3D quaternion coordinate system is now defined without its omnidirectionally alignable real axis.

$$H_0 = H_{[a=0]} = b \cdot \boldsymbol{i} + c \cdot \boldsymbol{j} + d \cdot \boldsymbol{k} \tag{13}$$

In this study, as a practical example for comparing 2D complex plane treatment and 3D quaternion coordinate system treatment, we will use a standard capacitive and inductive reactance situation in which resistance R and current I values are traditionally represented on the complex plane as applying along the real axis as represented on the left side of **Figure 5**, while the capacitive reactance C related to the induced electric field ***E*** is represented as being rotated along the negative side of the imaginary axis, while the inductive reactance L related to the induced magnetic field ***B*** is represented as being rotated along the positive side of the imaginary axis (left side of **Figure 7**), which causes them to apparently be offset by 180° with respect to each other (left side of **Figure 5**). Reference [28] provides very clear visual representations of the 3 representations in complex form of the RLC reactance equations – reproduced on the left side of **Figures 5, 6 and 7**.

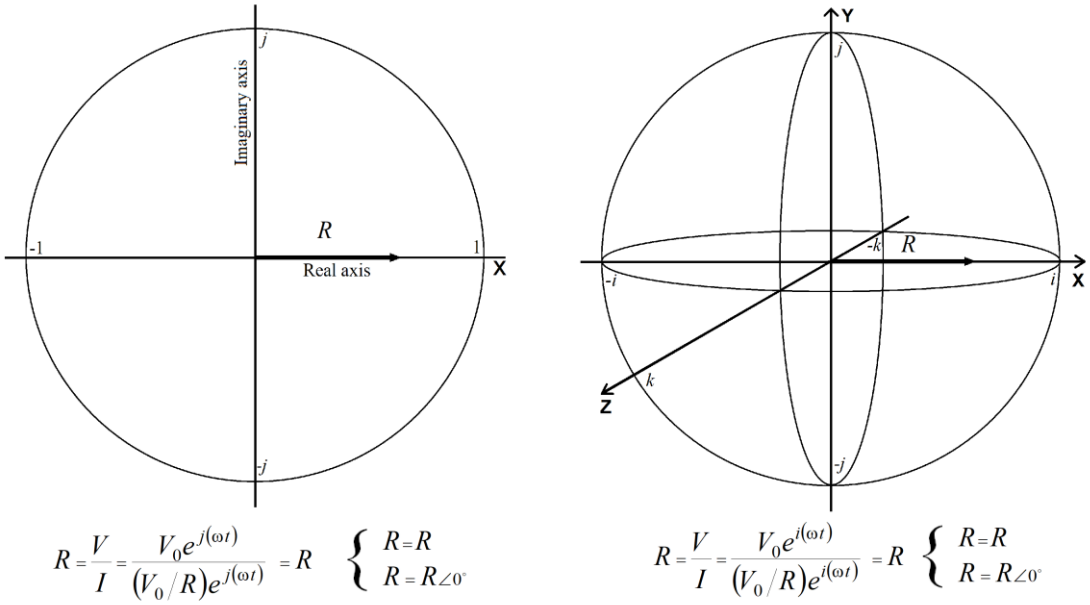

Figure 5: Resistance (Complex Form) – Comparison between 2D complex plane representation and 3D quaternion coordinate system representation.

We note from the right side representation of **Figure 5** that the resistance vector is still aligned along the x-axis, now mapped over by the ***i***=√-1=1∠0° unit vector in the quaternion coordinate system. The only change in the equations turns out to be that unit vector ***i*** now replaces unit vector ***j*** in the resistance equations.

Let us note that this replacement of unit vector ***j*** by ***i*** does not affect the numerical resolution of the equations in any way, since both unit vectors are equal to the same √-1 value. Some may argue that using ***i*** this may would be counterproductive, since ***j*** was chosen in electronic context to represent √-1 precisely to avoid confusion between *irrational number* symbol ***i*** and the standard symbol **I** used to represent current.

Noting that capitalized letter I is also being used as a symbol for current while small letter ***i*** is used for the irrational number in combination with context of use should be amply sufficient to avoid any confusion.

Let us now have a look at the comparative representations of the capacitive reactance complex forms (**Figure 6**):

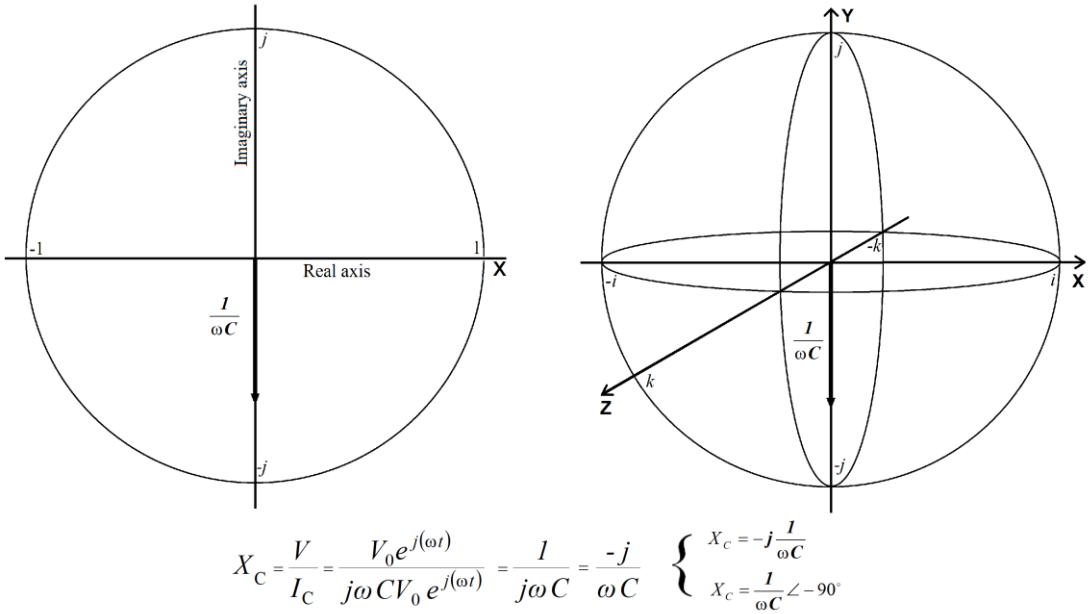

$$X_C = \frac{V}{I_C} = \frac{V_0 e^{j(\omega t)}}{j\omega C V_0 e^{j(\omega t)}} = \frac{1}{j\omega C} = \frac{-j}{\omega C} \quad \begin{cases} X_C = -j\frac{1}{\omega C} \\ X_C = \frac{1}{\omega C}\angle -90^\circ \end{cases}$$

Figure 6: Capacitive Reactance (Complex Form) – Comparison between 2D complex plane representation and 3D quaternion coordinate system representation.

In **Figure 6** we observe that no change whatsoever is to be noted between 2D complex plane representation and 3D quaternion coordinate system representation, given that the vertical axis of the complex plane was already identified with the $\boldsymbol{j}=\sqrt{-1}=1\angle 90°$ symbol. So the equations do not need to be modified.

A major change will be observed however for the impedance equation as shown in **Figure 7**. It is well established in electromagnetic theory and easily confirmable experimentally that the magnetic field about a wire, or wire coil, self-orients perpendicularly to the electric field ($\angle 90°$).

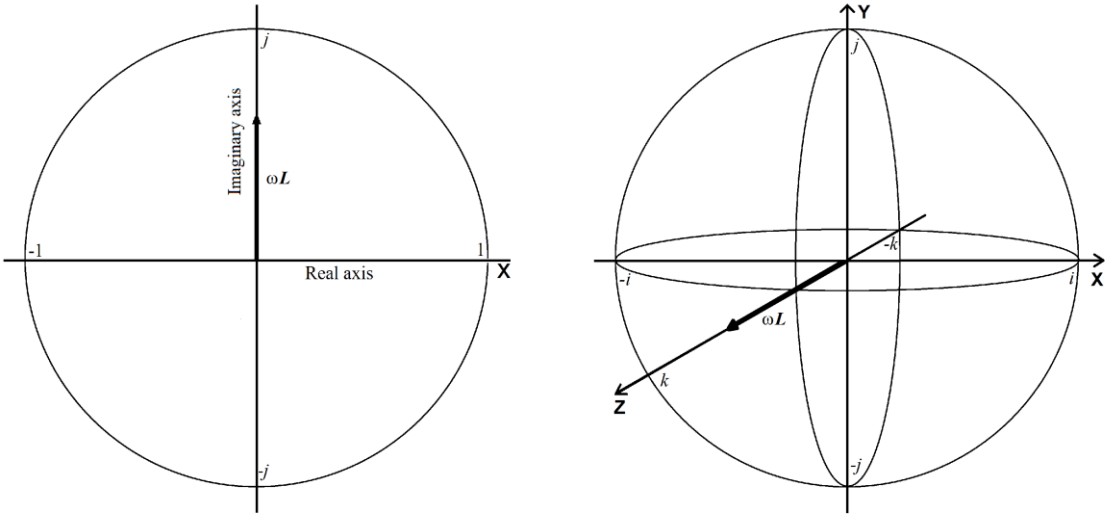

$$X_C = \frac{V}{I_L} = \frac{V_0 e^{j(\omega t)}}{\frac{V_0}{j\omega L} e^{j(\omega t)}} = j\omega L \quad \begin{cases} X_L = j\omega L \\ X_L = \omega L \angle 90^\circ \end{cases}$$

$$X_C = \frac{V}{I_L} = \frac{V_0 e^{k(\omega t)}}{\frac{V_0}{k\omega L} e^{k(\omega t)}} = k\omega L \quad \begin{cases} X_L = k\omega L \\ X_L = \omega L \angle 90^\circ \end{cases}$$

Figure 7: Inductive Reactance (Complex Form) – Comparison between 2D complex plane and 3D quaternion coordinate system representations.

It is indeed well established that when electrons are set in motion in a wire by applying voltage to it, a macroscopic magnetic ***B***-field instantly develops about the wire that can easily be directly detected with a very ordinary magnetic compass, and whose direction about the wire is very precisely perpendicular to the direction of motion of the flow of electrons in the wire.

The Einstein-de Haas and Barnett experiments carried out in the early 20th century [29] have clearly established that such a build up of a magnetic ***B***-field to macroscopically measurable level related to electron

flow motion is due to the addition of the individual local magnetic Δ***B***-fields of the carrying energy of each electron involved, which exist at the level of each electron in a rigid and permanently invariant 3-way perpendicular relation with their related Δ***E***-fields and Δ***K*** momentum energy, related to the well established ***E/B***=v vectorial cross-product relation of the ***E*** and ***B*** vectors as represented with **Figure 2**.

So given that the electron flow initiated by applying a voltage to the wire – involving of course countless electrons in the wire all starting to move in the same direction along the outer surface of the wire – will force their individual Δ***B*** magnetic fields to all align in additive parallel magnetic spin orientation perpendicularly to the direction of the motion of the electron flow.

It is also well established that the flow of electrons occurs at the surface of the wire, each moving negative electron remaining strongly attracted all along its progression to the closest positive atomic nucleus that it happens to pass by in the wire; that is, a direction of interaction between electrons and atomic nuclei that establishes the local electric Δ***E***-fields as being oriented perpendicular to both the direction of motion of the electrons flow at the surface of the wire on one hand, and to the direction of the macroscopic ***B***-field about the wire on the other hand.

This triple orthogonality, traditionally represented with **Figure 2** can now also be visualized within the triply orthogonal coordinate system of the Hamilton hypersphere, as illustrated on the right sides of **Figures 5, 6** and **7,** regrouped for comparison in **Figure 8**.

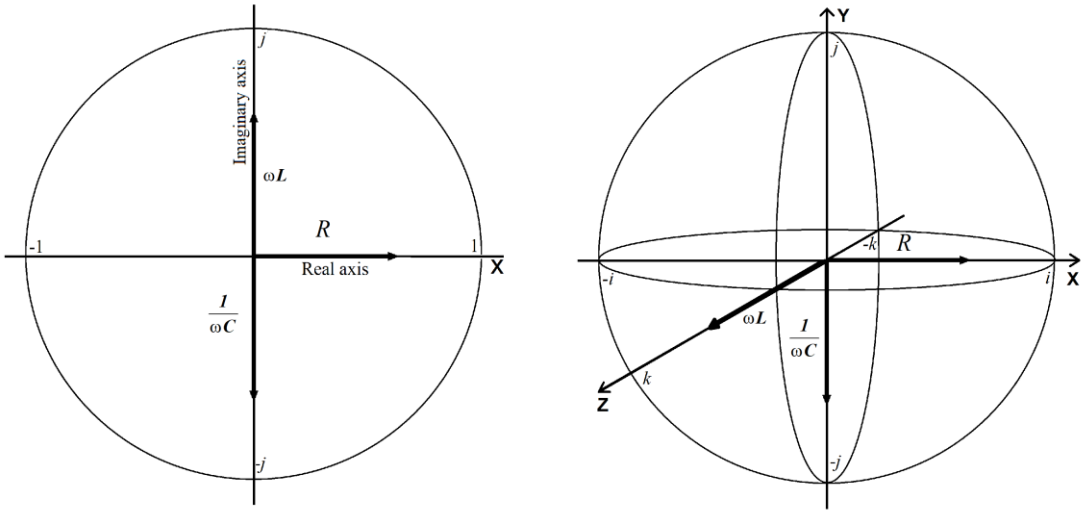

Figure 8: Comparative representations of the RLC system electromagnetic vectorial structure in the traditional 2D complex plane and in the 3D quaternion orthogonal coordinate system.

When comparing the traditional Cartesian coordinate system of **Figure 2** traditionally used in electromagnetic mechanics to represent the well established triply orthogonal electromagnetic relation with the representation of **Figure 8b**, the reader can certainly appreciate that the 3D quaternion orthogonal coordinate system representation is a more adequate representation of this vectorial relation than that of 2D complex plane.

So, an eventual upgrade of the complex forms of electronic LC and RLC equations from the 2D complex plane representation to the 3D quaternion coordinate system representation would have the benefit of vectorially representing the L-component related to the ***B***-field in LC and RLC systems at its true ∠90° offset angle with respect to the ***E***-field related C-component capacitance. The complex plane representation correctly represents the orthogonal relationship between the two L and C components being ∠90° out of phase with the ***i-x*** axis direction, but represents incorrectly the L and C components as being ∠180° out of phase with each other, in the only way that the 2D complex plane can represent them.

VI. DETAILED ANALYSIS OF THE 3D QUATERNION COORDINATE SYSTEM

Referring back again to Equation (13) that isolates the 3D quaternion coordinate system, involving the 3 perpendicular coordinates of the Hamilton hypersphere [b***i*** +c***j*** + d***k***], a few other characteristics of this coordinate system deserve a closer look. The first observation is that any vectorial cross-product of two of these unit vectors results in the reversal of the direction of application of the third unit vector that applies in the third perpendicular direction, as illustrated in **Figure 9**.

$$\boldsymbol{j}\times\boldsymbol{k}=\boldsymbol{k}\times\boldsymbol{j}=-1_i \qquad c\boldsymbol{j}\times d\boldsymbol{k}=d\boldsymbol{k}\times c\boldsymbol{j}=-b_i \tag{14}$$

$$\boldsymbol{i}\times\boldsymbol{k}=\boldsymbol{k}\times\boldsymbol{i}=-1_j \qquad b\boldsymbol{i}\times d\boldsymbol{k}=d\boldsymbol{k}\times b\boldsymbol{i}=-c_j \tag{15}$$

$$\boldsymbol{i}\times\boldsymbol{j}=\boldsymbol{j}\times\boldsymbol{i}=-1_k \qquad b\boldsymbol{i}\times c\boldsymbol{j}=c\boldsymbol{j}\times b\boldsymbol{i}=-d_k \tag{16}$$

$i=j=k=\sqrt{-1}$

$i^2=j^2=k^2=-1$

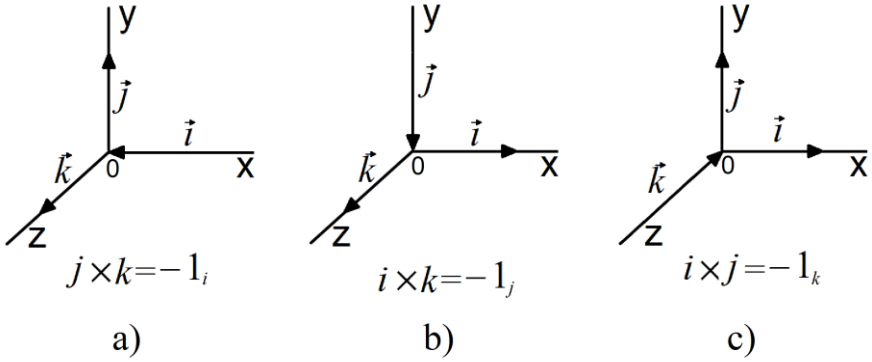

Figure 9: Illustration of the cross product of unit vectors defined by structure as ***i*=*j*=*k***=√-1=1∠90° resulting in the third unit vector reversing its direction of application.

Let us analyze the implications. Observing that the resultant perpendicular unit vector of each vectorial cross product is a negative *real* unit vector, this can only mean that whatever value will be related to this unit vector as a consequence of the cross product of the values related to the first two *complex* unit vectors will be applied in reverse, that is, towards the center of the triply orthogonal structure (**Figure 9**), given that it is defined as applying between the origin **0** and distance 1 from the origin.

With reference to Equation (14) and **Figure 9a**, this would involve that a vectorial cross product of values *c**j*** and *d**k*** would result in a reversed direction of application of the value related to the resulting reversed vector b_i; that a vectorial cross product of values *b**i*** and *d**k*** of Equation (15) and **Figure 9b** would result in a reversed direction of application of the value related to the resulting vector c_j; and that a vectorial cross product of values *b**i*** and *c**j*** of Equation (16) and **Figure 9c** would result in a reversed direction of application of the value related to the resulting vector d_k.

Consequently, if we were to locate a *coordinate reference system* identical to that of **Figure 8b**, with its unit vectors set defined as ***i*=*j*=*k***=√-1=1∠90° at the center-of-presence of an elementary particle, and if the *energy substance* of which this elementary particle is made was found to have characteristics that would allow it to oscillate between the two unit vector states whose cross product results in such a reversed direction of application of the resulting perpendicular unit vector, this would indeed clarify and confirm the direction of application of the value related to the reversed unit vector.

It so happens that the conditions that de Broglie identified in 1937 for localized electromagnetic photons following precise least action trajectories to obey Maxwell's equations [22], precisely involve that the energy substance of which these localized photons are made, as defined by Einstein in his first 1905 article [30], has to be such a substance, whose required characteristics were identified in References [10][11].

The conditions identified by de Broglie ([22], p.277) were that to satisfy at the same time the Bose-Einstein's statistic and Planck's Law, to perfectly explain the photoelectric effect while obeying Maxwell's equations and remain totally conform to the properties of Dirac's theory of complementary corpuscles symmetry, the localized photon could be explained only if it involves two particles, or half-photons of spin 1/2.

He added that such a complementary couple of particles is likely to annihilate at the contact of matter by relinquishing all of its energy, and that being made of two elementary particles of spin h/4π, it will obey the Bose-Einstein statistic as required by the precision of Planck's law for the black body, and finally that this model of the photon allows the definition of an electromagnetic field linked to the probability of annihilation of the photon, a field that obeys Maxwell's equations and has all the characteristics of electromagnetic light waves.

The characteristics identified in References [10][11] that the energy substance must have for localized electromagnetic photons to obey the whole set of conditions identified by de Broglie are *incompressibility*, *fluidity*, *elasticity* and *a-tendency-to-always-remain-in-motion.*

Coming back to this other conclusion by de Broglie quoted previously that the non-individuality of particles, the exclusion principle and exchange energy are three intimately related enigmas that are tied to the impossibility of exactly representing elementary physical entities within the frame of continuous three dimensional space – or more generally of continuous four dimensional space-time. This conclusion is tied to the impossibility of identifying any logical mechanical manner in which this energy substance could be set in

internal electromagnetic oscillation between the two states represented by the ***j*** and ***k*** unit vectors of the 3D Cartesian coordinate system within the restricted confines of normal 3D space, that would coherently explain their measurable frequencies.

Nor has it been possible to establish, within the restricted confines of normal 3D space, a logical mechanical manner that would explain how electromagnetic photons with energy in excess of 1.022 MeV, assumed to be massless, manage to split into a massive electron and positron pair, as discovered way back in the 1930's during Anderson's first detection of positrons in his bubble chamber [31], one occurrence of which was clearly recorded in FERMILAB experiment E-632 as analyzed in Reference [32], that was carried out in FERMILAB's 15 foot bubble chamber [33].

Nor was it possible to provide any mechanical explanation to the invariant unit electric charge of the electron and of the positron, nor of the fractional charges of the 3 scatterable inner components of protons and neutrons.

Nor has it been possible to provide a mechanical explanation for the relative *magnetic spin* interaction between charged electrons that enables them to pair up in attractive antiparallel orientation to establish covalent bonds between atoms despite their equal same sign repulsive electric charges, in pairs to fill electron orbitals in atoms and in free-moving Cooper pairs, and finally in relative default repulsive parallel spin orientation to prevent electrons from crashing into atomic nuclei in atoms.

Nor was it possible to establish in the restricted confines of normal 3D space a logical mechanical manner in which the 3-body structures of protons and neutrons could be stabilized as observed, with the proton being permanently stable, and the neutron becoming somewhat unstable when isolated, i.e., two structures that, to remain consistent with the electromagnetic nature of their scatterable triad subcomponents, must mechanically simultaneously rotate and translate in two directions perpendicular to each other about two perpendicular rotation/translation axes that intersect in the neutron structure, which explains its instability and do not intersect in the proton structure, which explains its stability, as analyzed in Reference [32].

To allow readers to more easily become aware of the unexpected internal state of motion of nucleons, the illustrations used in Reference [32] in context of the analysis and publication in 2013 of the 3-bodies internal structures of proton and neutron, are reproduced here as **Figure 10**, representing the scatterable charged electromagnetic sub-components involved only by their centers-of-presence, without illustrating their trispatial vector complexes, which have been made available in References [13][14] in context of the establishment of the common vector field of electromagnetic and kinematic mechanics [14].

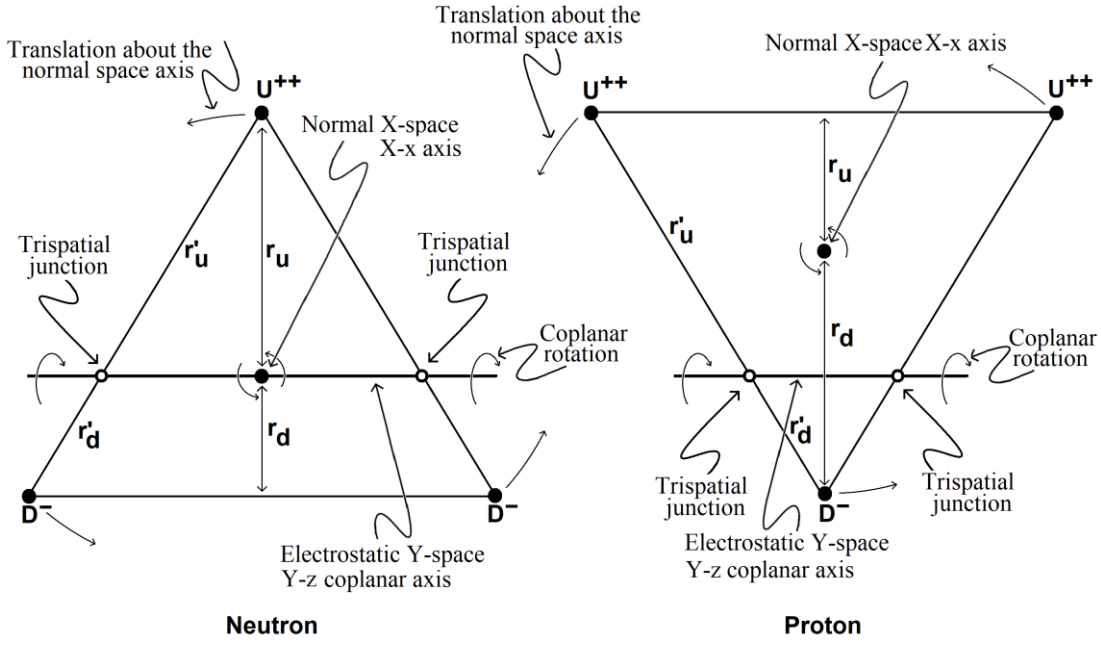

Figure 10: Rotation and translation axes of the proton and neutron internal scatterable subcomponents triads.

VII. THE TRISPATIAL GEOMETRY

First introduced in a popularization work in 1999 – that was republished in 2012 in E-book format [34] – the more extensive space geometry that de Broglie had sensed the need for was first proposed, that brought the solution to these mechanical processes that he had concluded were impossible to establish within the

confines of our normal 3D space, to then be presented in 2000 at Congress-2000 held in St Petersburg State University [23], and to finally be formally published in April 2013 in Reference [35].

This expanded space geometry allowed explaining the frequencies of localized photons by means of a mechanical oscillation of half a photon's energy between the ***E***-field state and the ***B***-field state in agreement with Maxwell's initial interpretation of the mutual reciprocating induction of both field on a plane transverse to its direction of motion, as analyzed in references [13][14].

It also allowed explaining how the total amount of energy of a moving photon of energy in excess of 1.022 MeV could convert to a pair of *massive* electron and positron by mechanically transferring all of its energy on a plane perpendicular to normal space [26].

It also allowed bringing a mechanical explanation to the problem impossible to resolve in normal 3D space of the nucleons internal triads rotating/translating about two axes perpendicular to each other, that intersect within the neutron structure, which explains its instability when isolated, but that do not intersect within the proton structure while remaining perpendicular to each other, which explains the total proton stability [32].

This expanded space geometry also allowed providing a mechanical explanation to the invariant unit electric charge of the electron and of the positron, and a mechanical explanation to the fractional charges of the 3 scatterable inner components of protons and neutrons, as analyzed in Reference [32].

It also provided a mechanical explanation to the relative *magnetic spin* interaction that allows charged electrons to pair up in attractive antiparallel orientation to establish covalent bonds between atoms despite their same sign equal repulsive electric charges, in pairs to fill electronic orbitals in atoms and in free-moving Cooper pairs, and finally in relative default repulsive parallel spin orientation to prevent electrons from crashing into atomic nuclei in atoms, as confirmed by the experiment that underlies the development of the trispatial geometry [20].

Briefly presented, this solution emerged from the long established invariant triple vectorial orthogonality of the vector cross product of the ***E***- and ***B***-fields vectors which is so fundamental in electromagnetism (**Figure 11a**). When the ***j*** and ***k*** minor unit vectors of *normal space* representing the ***E***- and ***B***-fields in classical electromagnetism are *expanded* into becoming fully developed major 3D vectorial spaces represented by ~~***J***~~ and ~~***K***~~ *major unit vectors*, each possessing its own internal ~~***ijk***~~ *minor unit vectors set*, a fully developed major 3D vectorial normal space, represented by a major unit vector ~~***I***~~, emerges by vectorial cross product of the majors vectors ~~***J***~~ and ~~***K***~~, that also maintains its usual internal set of minor ~~***ijk***~~ unit vectors (**Figures 11b** and **11c**).

This entirely new vectorial space geometry effectively allowed logically representing not only free moving photons according to de Broglie's conditions, but also to mechanically explain how such photons of sufficient energy can decouple into pairs of *massive* electron-positron [26], and also to mechanically explain how triads of sufficiently thermal electrons and positrons can accelerate to stabilize as the most energetic triads of elementary electromagnetic particles configurations that can exist in the universe, that is, protons and neutrons [32], and whose electromagnetic intensity of their new environment would explain the warping of their mass and charge characteristics towards their observed states.

The common punctual origin **0** of the three orthogonal vector spaces is then conceptualized as an infinitesimal volume *dV* through which the energy of a localized quantum, now perceived as a local quantity of physically existing energy substance, can now transit between the three spaces as if they were communicating vessels, to establish the state of equilibrium required by symmetry, and whose infinitesimal cross-section *ds* serves as a fulcrum against which half the energy of the quantum can apply its pressure to cause the other half to move in space – oscillating transversely in stationary mode on a plane perpendicular to the direction of this movement in space – when the local electromagnetic environment permits. Thus emerged, for visualization purposes, the 3x3D+1 augmented vector space underlying the trispatial model, with the +1 element of course representing the time dimension, which is analyzed in Reference [36].

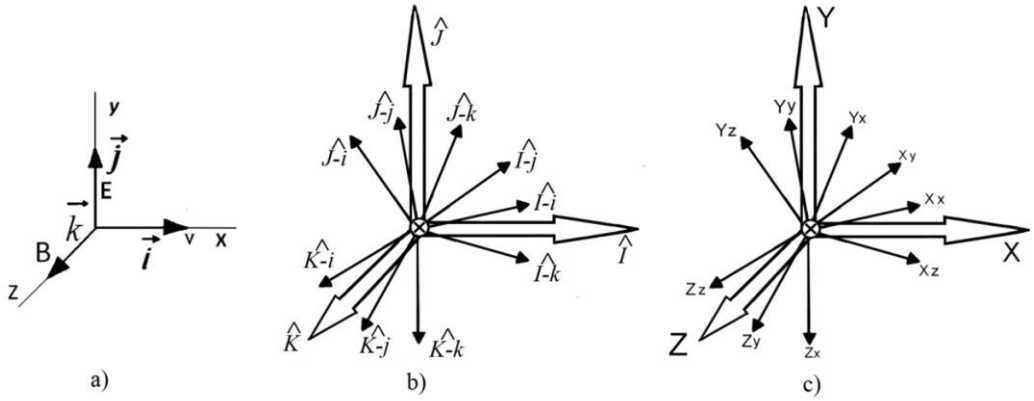

Figure 11: Major and minor unit vector sets applicable to the trispatial geometry.

The difficulty for us to mentally visualize more than 3 perpendicular dimensions at once is resolved by treating each of the major 3D vector spaces ***I J K*** as if they were folded 3-rib umbrellas meeting perpendicularly at their tips, and which, once folded, reduce the set of major 3x3D vector spaces to the basic 3D cross product vector representation of **Figure 11a**, and if the major unit vector set ***I***=***J***=***K***=1 is replaced by a major unit vector set ***I***=***J***=***K***=√-1=1∠90° in **Figure 11b**, then major unit vector ***I*** will reverse its direction of application when the cross product of major unit vectors ***J*** and ***K*** is applied (vectors ***J***×***K***=-1$_{\boldsymbol{I}}$) and the momentum energy related to unit vector ***I***=√-1=-1∠180°, will be shown to be correctly oriented to effectively apply its pressure against the infinitesimal *ds* surface as it propels the inert transversely oscillating energy present on the opposite side of the *ds* junction separating the three spaces, which would be consistent with the outcome of Equation (14) as illustrated with **Figure 9a**.

Simply opening the umbrellas one by one, allows visualization in sequence the motion of the energy substance as it circulates within each 3D vector space of the set.

The cross product of vectors ***j*** and ***k*** as traditionally established in the classical Cartesian coordinate system involving unit vectors ***i***=***j***=***k***=1 (**Figure 2**, reproduced as **Figure 11a**) seems to leaves the resulting vector as applying in the positive direction ***j***×***k***=1$_{\boldsymbol{i}}$, but that in reality leaves it undefined because a unit vector defined as ***i***=1 is not fundamentally directional while a *unit vector* defined as ***i***=√-1=-1∠180° is directional by structure, which clearly confirms its reverse direction of application, that his, for the element related to the now *real unit vector* (-1∠180°)$_{\boldsymbol{i}}$ to be geometrically represented as applying its pressure against the two elements represented by the two *complex unit vectors* ***j***×***k*** that are now involved in the related vectorial cross product.

From within real normal X-space, all energy present within complex electrostatic and magnetostatic Y- and Z-spaces at any given moment of each cycle of the electromagnetic frequency of the substance quantum involved will appear to possess both longitudinal and transverse inertia, that is, *omnidirectional inertia*. In other words, it will appear to possess *electromagnetic mass*. Metaphorically speaking, the energy present in these two extra complex spaces would behave as if it was captive inside some invisible *container* that will resist being pushed around from any direction from within real normal X-space, with the unidirectional momentum energy present in X-space exerting its pressure against its center-of-presence, as analyzed in References [10][11].

VIII. THE ELECTROMAGNETIC PHOTON

It happens to also be the case for the momentum component [$(hc/2\lambda)_x$ ***I i***] of the localized double-particle electromagnetic photon defined according to Louis de Broglie's conditions, that resulted in the establishment of its LC Equation (17). First published in 2004 in a popularization work [37] that was widely distributed in paperback format in numerous institutions' physics departments, this equation and its companion derivatives were then formally published in 2013 in Reference [35], then republished in 2016 in References [10][11] to explain all aspects of its ontological origin:

$$E\vec{I}\vec{i} = \left(\frac{hc}{2\lambda}\right)_X \vec{I}\vec{i} + \left[\ 2\left(\frac{e^2}{4C}\right)_Y (\vec{J}\vec{j}, \vec{J}\overleftarrow{j})\cos^2(\omega t) + \left(\frac{L\,i^2}{2}\right)_Z \overleftrightarrow{K}\ \sin^2(\omega t)\right] \qquad (17)$$

In which:

$$C = 2\varepsilon_0\alpha\lambda \qquad L = \frac{\mu_0\alpha\lambda}{8\pi^2} \qquad i = \frac{2\pi ec}{\alpha\lambda} \qquad (18)$$

as well as its ***E***- and ***B***-fields related counterpart, established according to the vectorial cross product defined with Equation (14), i.e. $c\boldsymbol{j} \times d\boldsymbol{k} = -b_{\boldsymbol{i}}$:

$$\mathrm{E}\,\vec{\mathrm{I}}\,\vec{\mathrm{i}} = \left(\frac{\mathrm{hc}}{2\lambda}\right)_{\mathrm{X}} \vec{\mathrm{I}}\,\vec{\mathrm{i}} + \left[2\left(\frac{\varepsilon_0 \mathbf{E}_{2\lambda}{}^2}{4}\right)_{\mathrm{Y}} (\vec{\mathrm{J}}\,\vec{\mathrm{j}}, \vec{\mathrm{J}}\,\overleftarrow{\mathrm{j}})\cos^2(\omega t) + \left(\frac{\mathbf{B}_{2\lambda}{}^2}{2\mu_0}\right)_{\mathrm{Z}} \overleftrightarrow{\mathrm{K}}\,\sin^2(\omega t)\right] \mathrm{V}_{2\lambda} \qquad (19)$$

In which:

$$\mathbf{E} = \frac{\pi e}{\varepsilon_0 \alpha^3 \lambda^2} \quad \mathbf{B} = \frac{\mu_0 \pi e c}{\alpha^3 \lambda^2} \quad \mathrm{V} = \frac{\alpha^5}{2\pi^2}\frac{\lambda^3}{2\pi^2} \qquad (20)$$

This triple orthogonal relation between the photon ***E***- and ***B***-fields, perpendicular to each other, also representing their L- and C-counterparts, propelled by its momentum energy Δ***K***, was illustrated with the left side image of **Figure 12** in References [13][14]:

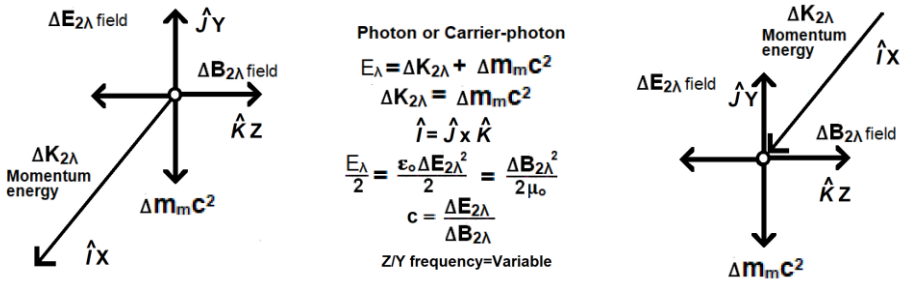

Figure 12: The trispatial vector complex of a photon or carrier-photon.

Of course, it could be argued in view of the fact that Equation (17) and (19) reveal that the ***i***x-vector related value *b* should be visually shown as directly applying pressure against the center-of-presence of the particle – coinciding with location **0** of the *reference coordinate system* – as tentatively illustrated with the right side representation of **Figure 12**, but given that this relation was always directly illustrated with the accompanying **Figure 13**, it was deemed that the left side representation carries the same vectorial idea while more clearly isolating the center of the triply orthogonal relation, that coincides with position **0** of the coordinate system, which is the common location of either the origin or the point of application of the whole set of vectors describing the inner structure of the de Broglie double-particle photon. From this perspective, Equation (16) for example, could be reformulated as follows:

$$\mathrm{E}\,\vec{\mathrm{I}}\,\vec{\mathrm{i}} = \left(0, (-\boldsymbol{I}//\boldsymbol{i})\frac{\mathrm{hc}}{2\lambda}\right)_{\mathrm{X}} + \left[\begin{array}{l} \left\{\left(0, (\boldsymbol{J}//\boldsymbol{j})\frac{\mathrm{e}^2}{4\mathrm{C}}\right) + \left(0, (\boldsymbol{J}// -\boldsymbol{j})\frac{\mathrm{e}^2}{4\mathrm{C}}\right)\right\}_{\mathrm{Y}} \cos^2(\omega t) + \\ \left\{\left(0, (\boldsymbol{K}//\boldsymbol{ijk})\frac{\mathrm{L\,i}^2}{2}\right) + \left(0, (\boldsymbol{K}// -\boldsymbol{i} -\boldsymbol{j} -\boldsymbol{k})\frac{\mathrm{L\,i}^2}{2}\right)\right\}_{\mathrm{Z}} \sin^2(\omega t) \end{array}\right] \qquad (21)$$

In which major unit vectors ~~***I***~~=~~***J***~~=~~***K***~~=√-1=1∠90° represent the 3 mutually orthogonal spaces of the trispatial geometry, and the three *minor unit vectors* sets ***i***=***j***=***k***=√-1=1∠90° represent the inner tridimensional coordinate systems within each space, and that vector representations (***I//i***, ***J//j***, ***J//-j***, ***K//ijk***, ***K//-i-j-k***) relate the inner space *minor unit vector*(*s*) subordinated to the local major unit vector ~~***I J***~~ or ~~***K***~~ of the space involved.

Vectorial configuration (***K//ijk***) represents the spherical expansion phase of the magnetic component of the photon's energy towards maximum presence within magnetostatic Z-space (**Figure 13b**), as it is in process of evacuating Y-space (**Figure 13a**), while vectorial configuration (***K//-i-j-k***) represents its spherical regression phase towards zero presence within magnetostatic Z-space (**Figure 13d**), as it is re-entering Y-space as twin charges moving away from each other within Y-space (**Figure 13e**) until maximum presence and separation in Y-space is reached, initiating the following cycle of its oscillation.

The relation between the polarizability of electromagnetic photons and the double-particle aspect of its ***E***-field state in Y-space, illustrated by **Figure 13a** is analyzed in References [10][11].

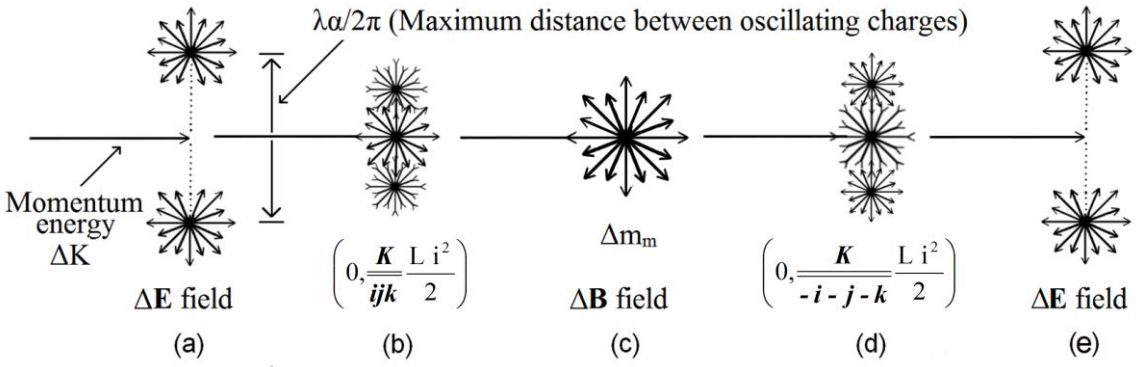

Figure 13: Representation of the stationary transverse oscillation cycle of the electromagnetic half-quantum of a free moving photon or of the carrier-photon of an electron.

We can now format Equation (17) according to the *quaternion coordinate reference system*'s cross product configuration of Equation (13), in which:

$$b=\left(\frac{hc}{2\lambda}\right)_{-X_I} \qquad c=2\left(\frac{e^2}{4C}\right)_{JY} \qquad d=\left(\frac{L\,i^2}{2}\right)_{KZ} \tag{22}$$

And finally:

$$E=\left|-b_X\right|+\left[c\boldsymbol{j}\cos^2(\omega t)+d\boldsymbol{k}\sin^2(\omega t)\right] \tag{23}$$

In which *–b* represents the momentum energy applying pressure against the center-of-presence of the particle visualized as an infinitesimal *ds* surface against which this pressure can be applied (Equation (14) and **Figure 9a**) as described in References [13][14], propelling at the speed of light in vacuum the *c* and *d* component of Equation (23) that are in constant oscillation on the ***JK*** plane perpendicular to its direction of motion in X-space, through the aforementioned infinitesimal volume ΔV that establishes the junction between the three vector spaces at point **0** of the cross product ***J*×*K*=*I***, in **Figure 11b**, that establishes the communicating vessels characteristic of the set.

IX. THE ELECTRON REST MASS AND ITS ELECTRIC CHARGE

One last vector cross product case remains to be put in perspective, which is illustrated with Equation (15) and **Figure 9b**.

This case concerns the mechanics of decoupling of a massless electromagnetic photon of 1.022 MeV or more into a pair of two massive particles of opposite electric sign with equal masses (m_0=8.18710414E-14 joules/c^2= 0.511 MeV/c^2) and equal electric charges (e=1.602176462E-19 Coulomb). The *rest mass* energy value of the electron or positron in mega-electronvolts (0.511 MeV) is obtained by dividing the mass value in joules by the value of the invariant electron unit charge (8.18710414E-14÷1.602176462E-19=0.5109989027 MeV).

The photon decoupling process involves the transfer of the momentum half of this electromagnetic photon to the same transverse orientation as its other half, as described with Equations (17) or (19), with a wavelength (λ) equal to half the Compton wavelength of the electron rest mass energy (λ_c=2.426310215E-12 meter) to the perpendicular orientation that already characterizes the electromagnetically oscillating half of the photon's energy.

The two LC equations describing the decoupled massive particles – an electron and a positron – were formally published in 2013 in Reference [26].

For the positron *rest mass*:

$$E\vec{\mathbf{0}}=m_e c^2\vec{\mathbf{0}}=\left[\frac{hc}{2\lambda_C}\right]_Y\vec{\mathbf{J}}\vec{\mathbf{i}}+\left(2\left[\frac{(e')^2}{4C_C}\right]_X(\vec{\mathbf{I}}\vec{\mathbf{j}},\vec{\mathbf{I}}\vec{\mathbf{j}})\cos^2(\omega t)+\left[\frac{L_C i_C^{\,2}}{2}\right]_Z\overleftrightarrow{\mathbf{K}}\sin^2(\omega t)\right) \tag{24}$$

and for the electron *rest mass*:

$$E\vec{\mathbf{0}}=m_e c^2\vec{\mathbf{0}}=\left[\frac{hc}{2\lambda_C}\right]_Y\vec{\mathbf{J}}\vec{\mathbf{i}}+\left(2\left[\frac{(e')^2}{4C_C}\right]_X(\vec{\mathbf{I}}\vec{\mathbf{j}},\vec{\mathbf{I}}\vec{\mathbf{j}})\cos^2(\omega t)+\left[\frac{L_C i_C^{\,2}}{2}\right]_Z\overleftrightarrow{\mathbf{K}}\sin^2(\omega t)\right) \tag{25}$$

In the same article, the ***E***- and ***B***-fields related equivalent equation for the electron *rest mass* was also proposed, mentioning that the equivalent equation for the positron was identical except for the orientation of its electrostatic Y-space minor unit vector [$\vec{\mathbf{J}}\vec{\mathbf{i}}$ for the positron and $\vec{\mathbf{J}}\vec{\mathbf{-i}}$ for the electron, as in equations (24) and

(25)]:

$$m_e c^2 \vec{\mathbf{0}} = \left[\frac{\varepsilon_0 \mathbf{E}^2}{2} V\right]_Y \vec{\mathbf{J}}\,\vec{\mathbf{i}} + \left[2\left(\frac{\varepsilon_0 \mathbf{V}^2}{4}\right)_X (\vec{\mathbf{I}}\,\vec{\mathbf{j}}, \vec{\mathbf{I}}\,\vec{\mathbf{j}})\cos^2(\omega t) + \left(\frac{\mathbf{B}^2}{2\mu_0}\right)_Z \overleftrightarrow{\mathbf{K}} \sin^2(\omega t)\right] V \qquad (26)$$

Vector $\vec{\mathbf{0}}$ related to the total energy of each massive particle refers to the fact that all of the energy of which the invariant *rest mass* of the electron and of the positron is physically oriented perpendicularly to *normal X-space*, meaning that none of its *rest mass* energy remains available to propel it in *normal space*, which directly relates to the discovery by Schrödinger referred to previously that the $\Psi_{(r,t)}$ component of his wave Equation (2) had to somehow be oriented perpendicularly with respect to its direction of motion as then hypothesized as being along the Bohr trajectory in the Bohr atom when in the ground state, which was established in his equation by the use of the perpendicular $\boldsymbol{i}=\sqrt{-1}=1\angle 90°$ *rotated unit vector*.

The analysis and description of the *neutrinic* energy component of the $()_x$ term of Equations (24), (25) and (26) is provided in Reference [38].

As put in perspective in References [13][14] and illustrated with **Figure 14**, a carrier-photon such as described with equations (17) and (19) needs to be associated with the *rest mass* of the electron or of the positron for them to be able to move in *normal space*.

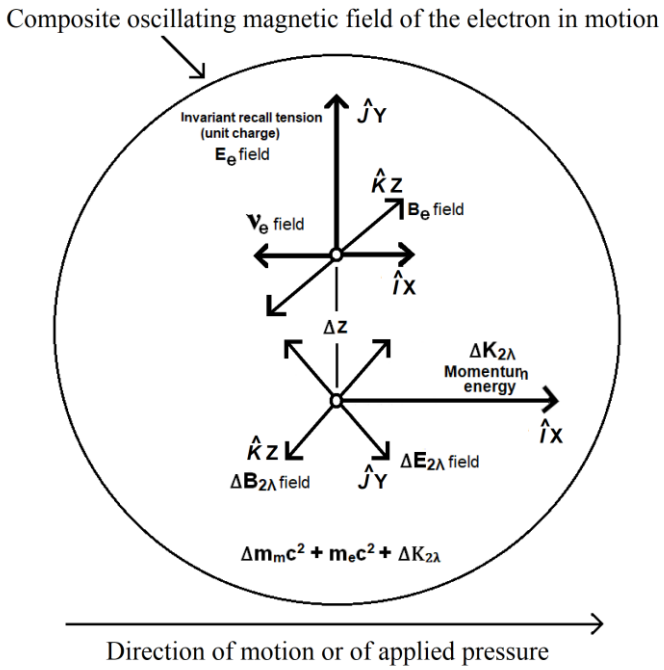

Figure 14: The trispatial vector complex of the *relativistic mass* of the electron in motion and of its momentum energy.

As put in perspective in References [13][14], it is the $\Delta\boldsymbol{K}$ momentum energy provided by this carrier-photon that the de Broglie Equation (1) and the Schrödinger Equation (2) allow calculating for each allowed orbital of the hydrogen atom, corresponding to the pilot wave concept introduced by de Broglie, that allows the particle to move in normal space.

Like all other LC and related ***E***/***B*** equations, including those describing the scatterable inner subcomponents of protons and neutrons [32], established in context of the trispatial geometry, Equations (24), (25) and (26) describing the *rest mass* of electrons and positrons can be reformulated to relate their local vector complexes to the origin **0** – or *ds* or *dV* junction location coinciding with their centers-of-presence – of each their local trispatial coordinate system (**Figure 11b**), as was done with Equation (21) for the two Equations (17) and (19), and as illustrated with their representations in **Figure 15**, in which the electron *charge tension vector* is oriented to the left by convention to represent its negative direction of application, while the positron *charge tension vector* is oriented to the right to represent its positive direction of application [26][13][14].

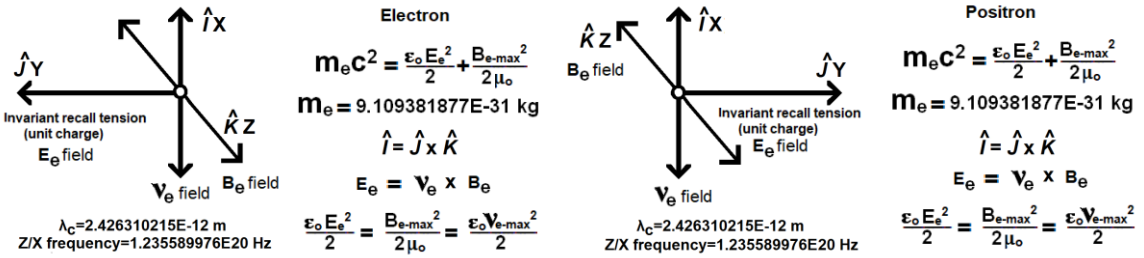

Figure 15: The trispatial vector complexes of the *invariant rest masses* of the electron and of the positron.

The trispatial geometry immediately sheds new light on the issue of the sign of electric charges, given that they would henceforth "live" within separate Y-space. The electric charge of elementary particles can now be represented as a vector with a negative, positive or null sign in Y-space. The charge of the electron would then amount to *invariant momentum pressure* in the negative direction along the Y-x axis, that of the positron to *invariant momentum pressure* in the positive direction along the Y-x axis, and the null sign of de Broglie's half-photons' charges would become explainable by these *variable opposite sign charges* oscillating in opposite directions on the Y-y/Y-z plane perpendicularly to the Y-x axis, a plane on which they are polarisable in any direction about the origin **0**, as put in perspective in References [10][11] and analyzed in References [39][40].

The recall tension aspect of the invariant electron and positron charges with respect to the Coulomb restoring force is analyzed in References [13][14]. The fractional charges of the scatterable inner subcomponents of protons and neutrons are analyzed in Reference [32].

Carefully comparing **Figure 13**, that represents the stationary transverse oscillation of electromagnetic photons or carrier-photons, with **Figure 16**, that represents the stationary transverse oscillation of the electron or positron *rest mass* energy, will allow observing that while half the energy of the photon oscillates between the double-particle ***E***-field state in Y-space and the single component ***B***-field state in Z-space, half of the energy of the electron or the positron oscillates rather between the double-particle ***ν***-field state in X-space and the single component ***B***-field state in Z-space.

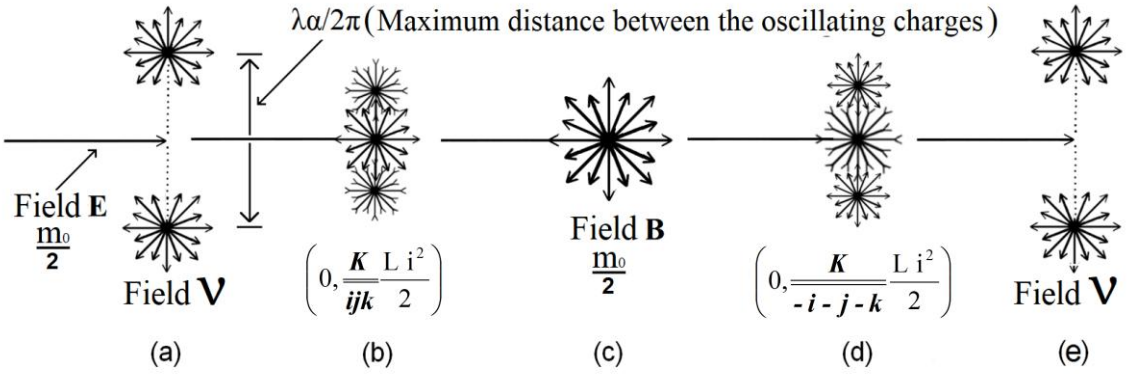

Figure 16: Representation of the cyclic oscillation of half the electron's rest mass energy between its magnetic ***B*** state and its neutrinic double-charge ***ν*** state, while the other half constitutes the invariant energy of its ***E***-field.

The same vectorial magnetic configuration (***K//ijk***) plus (***K//-i-j-k***) as for the electromagnetic photon (**Figure 13**), representing the spherical expansion and regression phases of the magnetic component of the electron's energy can be observed in Equation (26) and **Figure 16**. This relation between this behavior of the electron magnetically oscillating phase and the spin of the electron was discovered as an outcome of the experiment carried out in 1998 analyzed in Reference [20] that triggered the development of the trispatial geometry. The analysis of the related mechanical establishment of covalent molecular bounding, of the filling of electronic orbitals by electron pairs, of the generation of Cooper pairs, and of the related interpretation of the Stern-Gerlach experiment was made available in Reference [14].

As already mentioned, relating then **Figures 13** and **16** to their corresponding LC equations – Equation (17) for **Figure 13** and Equations (24) and (25) for **Figure 16** – it can be observed that while the energy of the photon oscillates between Y-space and Z-space, that of massive particles electron and positron oscillates between X-space and Z-space, as analyzed and put in perspective in Reference [26].

This is what brings attention back to the vectorial cross product of Equation (14) as illustrated with **Figure 9a** that structures Equation (17) so that the cross product of major unit vectors ***J*** and ***K*** results in the *momentum unit vector* of the photon being oriented towards its center-of-presence instead of away from it to correctly accounts for the fact that the momentum energy vector related to the resulting major unit vector $\boldsymbol{I}$=-$1_{\boldsymbol{I}}$

now applies its magnitude against the center-of-presence of the particle to propel it at the speed of light in vacuum, a speed of light due to the fact that the *propelled* amount of energy is *always exactly equal by symmetry* to the amount of *propelling* momentum energy in electromagnetic photons, as mathematically demonstrated in Reference [41].

Examining Equations (24) and (25) reveals that in the case of massive particles, subordinated to the major unit vector $\not{\mathbf{J}}$ of Y-space, is rather the cross product of *minor unit vectors* $\not{\mathbf{J}}\mathbf{j}$ and $\not{\mathbf{J}}\mathbf{k}$ which is involved, that results in the momentum minor unit vector $\not{\mathbf{J}}\mathbf{i}$ – on the plane Y-y/Y-x within Y-space – of the electron and the positron being oriented in opposite directions, applying pressure towards normal X-space for the positron and applying pressure away from normal space for the electron. In the trispatial geometry, it is this invariant pressure exerted in opposite directions towards and away from normal X-space which is measured as the invariant and opposite charges of the electron and of the positron. The pressure exerted by the fractional charges of the scatterable subcomponents of protons and neutrons is analyzed in Reference [32].

X. BEYOND THE FISSION AND FUSION OF ATOMIC NUCLEI

The trispatial geometry also allowed envisioning the possibility to generate energy levels far exceeding those of atomic nuclei fusion, as analyzed in References [42][43][44], by identifying mechanical means by which neutrons and protons could potentially be produced by causing triads of sufficiently thermal electrons and positrons to interact in such close proximity that they would mutually capture in e+ e+ e- and e- e- e+ triads, with insufficient energy to escape mutual interaction, as described in Reference [32].

From the conclusions drawn from the analysis of such triad formation in Reference [32], it became apparent that the 3 scatterable and charged subcomponents of protons and neutrons could simply be very normal electrons and positrons whose mass and charge characteristics simply were warped into these slightly increased rest masses and diminished fractional charges by the intensity of the electromagnetic environment that they stabilize into when reaching these final equilibrium state, that is, the most intense stable energy levels that exist at the subatomic level of magnitude in the universe.

The newly created energy liberated by each such nucleogenesis occurrence would amount to three bremsstrahlung photons of 155 MeV each, for a total of 465 MeV, plus a stable adiabatically generated relativistic unreleasable mass increase of 938 - 1.533 = 936.467 MeV/c^2, for a grand total energy gain of 1401.467 MeV, that is, 1,401,467,000 eV or 2.245E-10 Joules [32], which is 34.35 million times more energy than the 40.8 eV gained from the initial irreversible adiabatic acceleration of a newly created electron to the least action orbital of a hydrogen atom [42][43].

To make certain at the time that the description of this possibility would remain on permanent formal record, it was decided in 2015 to register a PCT application at the *World Intellectual Property Organization* (WIPO) for assessment and to apply for patents in Canada and in the US for identified potential means of achieving such nucleons generation, even if these possibilities were too far removed from current established physics theories to be accepted.

Consequently, these processes, summarily described with **Figures 17**, **18** and **19** are now in the public domain and their full description and justifications are now permanently available on the WIPO site as well as in the Patent databases of Canada and of the United States [45][46][47], at the disposal of anyone who wishes to investigate and potentially use them.

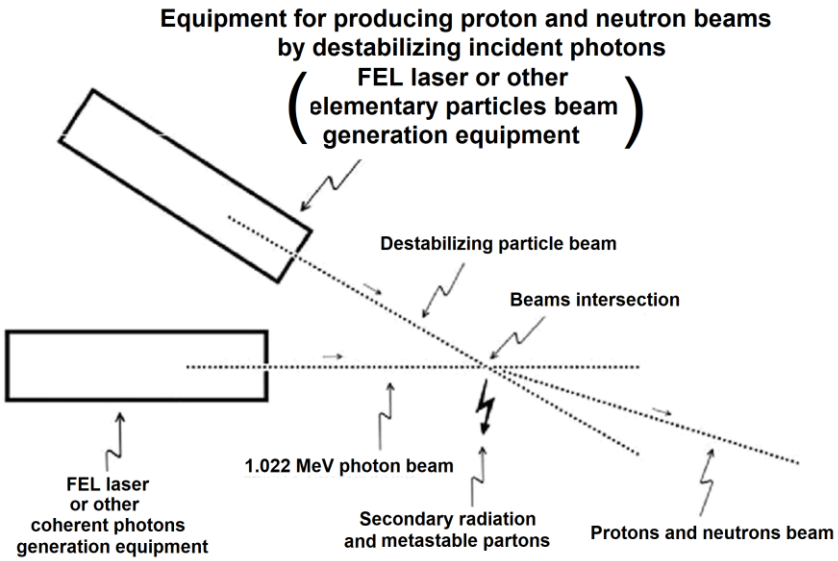

Figure 17: Schematic illustration of a particle beam generating equipment for generating protons and neutrons from destabilizing photons each having 1.022 MeV energy.

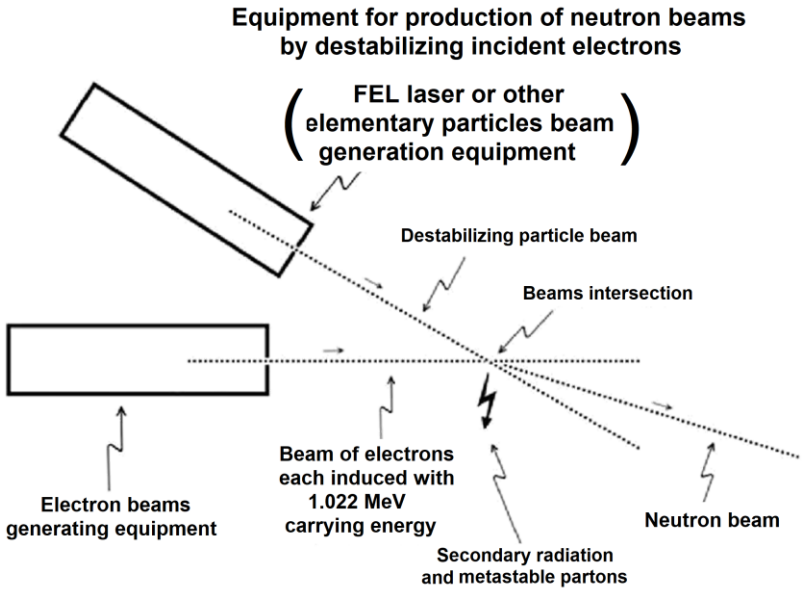

Figure 18: Schematic illustration of a particle beam generating equipment for generating neutrons by destabilizing electrons each having 1.022 MeV carrying energy.

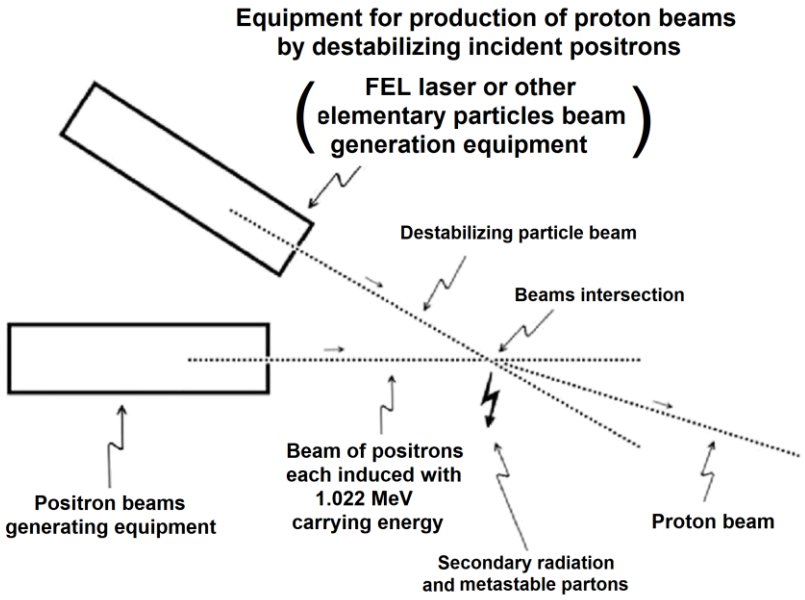

Figure 19: Schematic illustration of a particle beam generating equipment for generating protons from destabilizing positrons each having 1.022 MeV carrying energy

XI. CONCLUSION

With respect to Schrödinger's Equation (2), it can be observed that the use of complex numbers to account for the perpendicular orientation of the *rest mass energy* of the electron on the 2D complex plane with respect to its assumed direction of motion along the mean Bohr trajectory correctly represents de Broglie's non-relativistic Equation (1), given that the *classical rest mass* of the electron was perceived as having no internal structure, as analyzed in Reference [48] and that representing it with the single quantity represented by $\Psi_{(r,t)}$ harmoniously oscillating about the mean Bohr radius correctly accounted for the non-relativistic nature of the original de Broglie equation. Schrödinger's equation was eventually upgraded to full relativistic status by Dirac.

With regard to using complex numbers in the analysis of sinusoidally driven electronic circuitry, typically involving RLC or LC systems, made of wire coils and capacitors, we observed that the vectorial orientation of the L and C components of these systems can be correctly represented in the complex plane with respect to the real axis, since both L and C are represented as perpendicular to the direction of the real axis in the 2D complex plane, but that it is not possible to represent them otherwise than in opposition by 180° (**Figure 8a**), contrary to their known 90° mutual vectorial orientation in electromagnetic theory, which can be seen to be better represented within the *3D* quaternion coordinate system (**Figure 8b**).

With this analysis of the 2D complex plane illustrated with **Figure 3**, we rediscover Vessel's conclusion that in *complex number* a+***i***b, $\boldsymbol{i}=\sqrt{-1}=1\angle 90°$ is in reality a *directed unit vector* of magnitude 1 that rotates the direction of the magnitude of *b* by 90° with respect to the relative orientation of magnitude *a*.

From the analysis of the quaternion hypersphere illustrated with **Figure 4**, we observe that each unit vector of the 3D *directed unit vector sets* $\boldsymbol{i}=\boldsymbol{j}=\boldsymbol{k}=\sqrt{-1}=1\angle 90°$ and $\boldsymbol{i}^2=\boldsymbol{j}^2=\boldsymbol{k}^2=-1=1\angle 180°$ have the same rotation properties with respect to the 2D complex plane established by the other two *directed unit vectors* of the sets and with respect to magnitude *a* in *hypercomplex number* $a + b\boldsymbol{i} + c\boldsymbol{j} + d\boldsymbol{k}$.

When we isolate the directed 3D *unit vector complex* $\boldsymbol{i}=\boldsymbol{j}=\boldsymbol{k}=\sqrt{-1}=1\angle 90°$ of the quaternion and analyze it further, we observe that $\boldsymbol{i}^2=\boldsymbol{j}^2=\boldsymbol{k}^2=-1=1\angle 180°$ is the exact equivalent of the traditional 3D Cartesian unit vector set $\boldsymbol{i}=\boldsymbol{j}=\boldsymbol{k}=1$, in which $\angle\theta$ is undetermined, but that multiplying a Cartesian vector by -1 also reverses by 180° the direction of application of the Cartesian vector.

This means that fundamentally, the traditional Cartesian 3D *unit vector*s set $\boldsymbol{i}=\boldsymbol{j}=\boldsymbol{k}=1$which are perpendicular only *by definition* to each other could be potentially replaced with the *complex unit vector* set $\boldsymbol{i}=\boldsymbol{j}=\boldsymbol{k}=\sqrt{-1}=1\angle\theta=|1|$ in which the *unit vectors* are perpendicular *by structure* to each other and in which |1| is the absolute length of all unit vectors, that can take qualifying angular rotation values $|1|=1\angle\theta=1\angle 0°$ or $|1|= 1\angle\theta=1\angle 90°$ or $|1|= 1\angle\theta=1\angle 180°$, or remain unspecified with value |1|= 1 depending on the contextual mathematical requirement, then defaulting to $|1|=1=1\angle 0°$, in agreement with the traditional 3D set of Cartesian unit vectors $\boldsymbol{i}=\boldsymbol{j}=\boldsymbol{k}=1$.

The interest of this approach would be that the reversal of the direction of application of the third vector of an electromagnetic vectorial cross product such as represented with Equations (14), (15) and (16), related to the vectorial configurations of **Figures 9a**, **9b** and **9c**, would become a mathematical possibility

which is currently absent from our mathematical tool box if the unit vector set $\boldsymbol{i}=\boldsymbol{j}=\boldsymbol{k}=\sqrt{-1}=1\angle\theta=|1|$ that are mutually perpendicular *by structure* became used in electromagnetic mechanics instead of the current 3D Cartesian unit vectors set $\boldsymbol{i}=\boldsymbol{j}=\boldsymbol{k}=1$ that are perpendicular to each other *only by definition.*

REFERENCES

[1] Renou, MO., Trillo, D., Weilenmann, M. *et al*. (2021) *Quantum theory based on real numbers can be experimentally falsified*. *Nature* **600**, 625–629 (2021). https://doi.org/10.1038/s41586-021-04160-4.
https://www.nature.com/articles/s41586-021-04160-4

[2] Ming-Cheng Chen, Can Wang, *et al*. (2022) *Ruling Out Real-Valued Standard Formalism of Quantum Theory*. Phys. Rev. Lett. 128, 040403 – Published 24 January 2022. https://doi.org/10.1103/PhysRevLett.128.040403.
https://journals.aps.org/prl/abstract/10.1103/PhysRevLett.128.040403

[3] Padavic-Callaghan, K. (2022) *Complex numbers are essential in quantum theory, experiments reveal*. Quantum Mechanics. Research update. 11 Jan 2022.
https://physicsworld.com/a/complex-numbers-are-essential-in-quantum-theory-experiments-reveal/

[4] Nahim, P.J. (1998). *An Imaginary Tale – The Story of √-1*. Princeton University Press. New Jersey.

[5] Danielewski, M. and Sapa, L. (2020) Foundations of the Quaternion Quantum Mechanics. *Entropy* **2020**, *22*(12), 1424; https://doi.org/10.3390/e22121424.
https://www.mdpi.com/1099-4300/22/12/1424

[6] Graydon, M. (2011) Quaternions and Quantum Theory. UWSpace. *http://hdl.handle.net/10012/6168*.
https://uwspace.uwaterloo.ca/bitstream/handle/10012/6168/Graydon_Matthew.pdf?sequence=1&isAllowed=y

[7] Dunning-Davies, J. and Norman, R. (2020) *Deductions from the Quaternion Form of Maxwell's Electromagnetic Equations*. Journal of Modern Physics, **11**, 1361-1371. doi: 10.4236/jmp.2020.119085.
https://www.scirp.org/journal/paperinformation?paperid=102987

[8] Hong, I.K. and Kim, C.S. (2019) *Quaternion Electromagnetism and the Relation with 2*-Spinor *Formalism*. arXiv:1902.09773v2 [physics.class-ph].
https://arxiv.org/pdf/1902.09773.pdf

[9] Sears, F., Zemansky, M. and Young, H. (1984) *University Physics*, 6th Edition, Addison Wesley.

[10] Michaud, A. (2016) *On De Broglie's Double-particle Photon Hypothesis*. J Phys Math 7: 153. doi:10.4172/2090-0902.1000153.
https://www.hilarispublisher.com/open-access/on-de-broglies-doubleparticle-photon-hypothesis-2090-0902-1000153.pdf

[11] Michaud, A. (2021) *De Broglie's Double-Particle Photon*. In: Dr. Jelena Purenovic, Editor. Newest Updates in Physical Science Research Vol. 4, 63–102. https://doi.org/10.9734/bpi/nupsr/v4/1979F
https://stm.bookpi.org/NUPSR-V4/article/view/1642

[12] Resnick, R., Halliday, D. (1967) *Physics*. John Wyley & Sons, New York.

[13] Michaud, A. (2023) *Introduction to Synchronized Kinematic and Electromagnetic Mechanics*, Journal of Modern Physics, **14**, 876-932. doi:
10.4236/jmp.2023.146051.https://www.scirp.org/pdf/jmp_2023053016192489.pdf

[14] Michaud, A. (2023) *Electromagnetic and Kinematic Mechanics Synchronized in their Common Vector Field: A Mathematical Relation*, Journal of Modern Physics, **14**, 876-932. doi: 10.4236/jmp.2023.146051.
https://www.scirp.org/pdf/jmp_2023053016192489.pdf

[15] De Broglie, L. (1925) *Recherche sur la théorie des quanta*, Annales de Physique, Masson & Cie, Éditeurs. Paris.
https://theses.hal.science/file/index/docid/47078/filename/tel-00006807.pdf

[16] De Broglie, L. (2021) *Research on the Theory of Quanta*, Minkowski Institute Press. Edited by Vesselin Petkov. Montreal. Canada. https://www.amazon.ca/Research-Theory-Quanta-Louis-Broglie/dp/1927763983?asin=1927763983&revisionId=&format=4&depth=1

[17] Schrödinger, Erwin *(1982). Collected Papers on Wave Mechanics (3rd ed.). American Mathematical Society. ISBN 978-0-8218-3524-1.*

[18] Michaud, A. (2018) *The Hydrogen Atom Fundamental Resonance States*. Journal of Modern Physics, 9, 1052-1110. doi: 10.4236/jmp.2018.95067.

https://www.scirp.org/journal/paperinformation.aspx?paperid=84158

[19] Michaud, A. (2020) *An Overview of The Hydrogen Atom Fundamental Resonance States*. In: Dr. Mohd Rafatullah, editor. New Insights Into Physical Science Vol. 6. West Bengal, India: Book Publisher International. 2020.

http://bp.bookpi.org/index.php/bpi/catalog/book/265

[20] Michaud, A. (2013) *On The Magnetostatic Inverse Cube Law and Magnetic Monopoles*. International Journal of Engineering Research and Development e-ISSN: 2278-067X, p-ISSN: 2278-800X. Volume 7, Issue 5. pp. 50-66.

[21] Eisberg, R., and Resnick, R. (1985) *Quantum Physics of Atoms, Molecules, Solids, Nuclei, and Particles.* 2nd Edition, John Wiley & Sons, New York.

[22] De Broglie, L. (1993) *La physique nouvelle et les quanta*, Flammarion, France 1937, 2nd Edition 1993, with new 1973 Preface by Louis de Broglie. ISBN: 2-08-081170-3.

[23] Michaud, A. (2000) *On an Expanded Maxwellian Geometry of Space.* Proceedings of Congress-2000 – Fundamental Problems of Natural Sciences and Engineering. (2000) Volume 1, St.Petersburg, Russia, pages 291-310.

https://www.researchgate.net/publication/357527119_On_an_Expanded_Maxwellian_Geometry_of_Space

[24] Marmet, P. (2003) *Fundamental Nature of Relativistic Mass and Magnetic Fields*. International IFNA-ANS Journal, No. 3 (19), Vol. 9. Kazan State University.

http://www.newtonphysics.on.ca/magnetic/index.html

[25] Michaud, A. (2022) *Demystifying the Lorentz Force Equation*. Journal of Modern Physics, Vol.13 No.5, May 2022, **DOI:** 10.4236/jmp.2022.135046

https://www.scirp.org/pdf/jmp_2022053015080692.pdf

[26] Michaud, A. (2013) *The Mechanics of Electron-Positron Pair Creation in the 3-Spaces Model.* International Journal of Engineering Research and Development e-ISSN: 2278-067X, **p**-ISSN: 2278-800X. Volume 6, Issue 10. pp. 01-10.

http://ijerd.com/paper/vol6-issue10/F06103649.pdf

[27] Gélinas, R. & Lambert, M. (1988) *Éléments d'analyse complexe*. Presses de l'Université du Québec. Canada. ISBN 2-7605-0488-3.

[28] Scherz, P. (2007) *Practical Electronics for Inventors – Second Edition*. McGraw Hill. New York.

[29] Michaud, A. (2013) *On the Einstein-de Haas and Barnett Effects*, International Journal of Engineering Research and Development. e-ISSN: 2278-067X, p-ISSN: 2278-800X, www.ijerd.com Volume 6, Issue 12 (May 2013), PP. 07-11.

http://ijerd.com/paper/vol6-issue12/B06120711.pdf

[30] Einstein, A. (1905a) *Über einen die Erzeugung und Verwandlung des Lichtes betreffenden heuristischen Gesichtspunkt*. *Annalen der Physik*, vol. 17, n° 6, 1905, p. 132–148. (DOI 10.1002/andp.19053220607,

https://onlinelibrary.wiley.com/doi/epdf/10.1002/andp.19053220607

http://users.physik.fu-berlin.de/~kleinert/files/eins_lq.pdf

[31] Anderson, C.D. (1933) *The Positive Electron*, California Institute of Technology, Pasadena, California (Received February 28, 1933).

https://journals.aps.org/pr/pdf/10.1103/PhysRev.43.491

[32] Michaud, A. (2013) *The Mechanics of Neutron and Proton Creation in the 3-Spaces Model*. International Journal of Engineering Research and Development. e-ISSN: 2278-067X, p-ISSN : 2278-800X, Volume 7, Issue 9. pp. 29-53.

http://ijerd.com/paper/vol7-issue9/E0709029053.pdf

[33] Bodnarczuk, M.-W., Editor. (1988) *Reflections on the 15 Foot Bubble Chamber*. Fermi National Accelerator Laboratory Batavia, Illinois.

https://lss.fnal.gov/archive/misc/fermilab-misc-1988-01.pdf

[34] Michaud, A. (1999/2012). *Theory of Discrete Attractors*, SRP Books. Smashwords. ISBN: 9780988052727.

https://www.smashwords.com/books/view/159189

[35] Michaud, A. (2013) *The Expanded Maxwellian Space Geometry and the Photon Fundamental LC Equation*. International Journal of Engineering Research and Development, e-ISSN: 2278-067X, p-ISSN: 2278-800X. Volume 6, Issue 8, pp. 31-45**.**

http://ijerd.com/paper/vol6-issue8/G06083145.pdf.

[36] Michaud, A. (2021) *Our Electromagnetic Universe*. In: Dr. Mohd Rafatullah, Editor. Newest Updates in Physical Science Research Vol. 12. 23 July 2021, Page 64-82.

https://doi.org/10.9734/bpi/nupsr/v12/11459D

[37] Michaud, A. (2004). *Expanded Maxwellian Geometry of Space*. 4th Edition, SRP Books, Smashwords. ISBN: 978-0-988-05274-1.

https://www.smashwords.com/books/view/163704

[38] Michaud, A. (2013) *The Mechanics of Neutrinos Creation in the 3-Spaces Model*. International Journal of Engineering Research and Development. e-ISSN: 2278-067X, p-ISSN: 2278-800X. Volume 7, Issue 7, pp.01-08.

http://www.ijerd.com/paper/vol7-issue7/A07070108.pdf

[39] Michaud, A. (2017) *The Last Challenge of Modern Physics*. J Phys Math 8: 217. doi: 10.4172/2090-0902.1000217**.**

https://www.hilarispublisher.com/open-access/the-last-challenge-of-modern-physics-2090-0902-1000217.pdf

[40] Michaud, A. (2021) *The Last Challenge of Modern Physics: Perspective to Concept and Model Analysis*. In: Dr. Jelena Purenovic, Editor. Newest Updates in Physical Science Research Vol. 4, 1–29.

https://stm.bookpi.org/NUPSR-V4/article/view/1640

[41] Michaud, A. (2013) *From Classical to Relativistic Mechanics via Maxwell,* International Journal of Engineering Research and Development, e-ISSN: 2278-067X, p-ISSN: 2278-800X. Volume 6, Issue 4. pp. 01-10.

https://www.researchgate.net/publication/282353551_From_Classical_to_Relativistic_Mechanics_via_Maxwell

[42] Michaud, A. (2013) *Inside planets and stars masses.* International Journal of Engineering Research and Development. e-ISSN: 2278-067X, p-ISSN: 2278-800X. Volume 8, Issue 1. pp. 10-33.

http://ijerd.com/paper/vol8-issue1/B08011033.pdf

[43] Michaud, A. (2016) *On Adiabatic Processes at the Elementary Particle Level*. J Phys Math 7: 177. doi:10.4172/2090-0902.1000177.

https://projecteuclid.org/journals/journal-of-physical-mathematics/volume-7/issue-2/On-Adiabatic-Processes-at-the-Elementary-Particle-Level/10.4172/2090-0902.1000177.full

[44] Michaud, A. (2021) *On Adiabatic Processes at the Subatomic Level*. In: Dr. Jelena Purenovic, Editor. Newest Updates in Physical Science Research Vol. 4, 30–62. https://doi.org/10.9734/bpi/nupsr/v4/1978F

https://stm.bookpi.org/NUPSR-V4/article/view/1641

[45] Michaud, A. (2015) *WO2017041162 – Neutron and Proton Generating processes*. International Application No. PCT/CA2016/000201. World Intellectual Property Organization (WIPO).

https://patentscope.wipo.int/search/en/detail.jsf?docId=WO2017041162&recNum=1&maxRec=&office=&prevFilter=&sortOption=&queryString=&tab=PCT+Biblio

[46] Michaud, A. (2018) *Patent application CA 2997508 for Neutron and Proton Generating Processes*. Canadian Patent Database.

https://www.ic.gc.ca/opic-cipo/cpd/eng/patent/2997508/summary.html?type=number_search&tabs1Index=tabs1_1

[47] Michaud, A. (2018) *Patent application US-20180261348-A1 - Neutron and proton generating processes*. United States Patent Application Publication.

https://ppubs.uspto.gov/dirsearch-public/print/downloadPdf/20180261348

[48] Michaud, A. (2020) *Gravitation, Quantum Mechanics and the Least Action Electromagnetic Equilibrium States*. In: Amenosis Lopez, editor. Prime Archives in Space Research. Hyderabad, India: Vide Leaf. 2020.

https://videleaf.com/gravitation-quantum-mechanics-and-the-least-action-electromagnetic-equilibrium-states/